

Swiss-Norwegian Foundation for Research with X-Rays

Annual Report 2024

Contents

General Remarks	4
Introduction.....	5
ESRF highlights from SNBL.....	6
X-ray diffraction sheds light on CO ₂ -activated breathing-caloric materials for efficient refrigeration.....	7
<i>Operando</i> X-ray spectroscopy reveals insights into the stability of novel catalysts for CO ₂ reduction	10
<i>Operando</i> X-ray analysis of nickel gallium catalysts for CO ₂ hydrogenation to methanol.....	13
X-ray spectroscopy reveals particle size-dependent selectivity in cobalt CO ₂ hydrogenation catalysts	16
Research results from users enabled by the BM31 upgrade	17
(De)sodiation Mechanism of Bi ₂ MoO ₆ in Na-Ion Batteries Probed by Quasi-Simultaneous Operando PDF and XAS.....	18
Nucleation-Mediated Structure Selection Kinetics of Self-assembled Cobalt Nanoparticles in Solution and Catalytic State Formation	21
SNBL's staff research impacting the larger synchrotron community.....	24
Development of theoretical aspects of modern synchrotron diffraction geometries.....	24
Unravelling the components of diffuse scattering using deep learning	26
Success story: SNBL's software on diffuse scattering using deep learning applied to a user case.....	27
SNBL's Outreach	28
Spotlight article on the ESRF frontpage	28
Julian Walker wins Sten and Ingrid Ahrlands price	31
Aram Bugaev wins the ESRF Young Scientist Award 2025	33
Swiss Summer School on Diffraction and Crystallography, BM01-ESRF	35
Summer school success stories	36
Summer school success stories continued.....	38
SNBL's international review,	40
Scientific output and usage analysis.....	45
Impact Factors 2024	45
Summery Impact Factors 2019-2024	47
Research Areas 2024	48
Scientific output Partner countries 2024	49
SNBL Scientific output Partner countries 2019-2024.....	50
Intensive use of Swiss public ESRF beamtime on BM31	51
Involvement of industry in SNBL's 2024 publication output.....	54
Publication list 2024	59

General Remarks

The year 2024 is the twenty first year of the SNX Foundation.

The accounting is supervised by OPTIMA COMPTA, in Seyssinet-Pariset, in Isère, for the two French associations, and by BfB Fidam Fiduciaire in Renens VD for the SNX Foundation. AUDICT FIDUCIAIRE in Lausanne audits the accounts.

These legal frameworks contribute to the smooth running of the collaborations and to the successful scientific work done at the Swiss Norwegian Beam Lines at ESRF.

The activities of the SNX Foundation are carried out at the European Synchrotron Radiation Facility (ESRF) in Grenoble and comprise the operation and up-grade of two beam line branches, called the Swiss-Norwegian Beam Lines (SNBL).

Introduction

This report covers the year 2024, the fourth and final of the 4-year contract (2021-2024) between the Swiss partner, the École Polytechnique Fédérale de Lausanne (EPFL) and for Norway the Norwegian University of Science and Technology (NTNU), a new contract has been signed for next period (2025-2028).

The user program has been successfully continued in 2024, moreover the major upgrade program, spanning over the 4-year contract period, is now positively impacting the scientific output. This plan foresees that on BM01, Bragg diffraction, diffuse and small angle scattering, for single crystal, thin films and powder samples will become available. On BM31 the combined diffraction and X-ray absorption experiments setup is completed with Total Scattering and improvements in time and space resolution for all techniques. The BM01 phase 2 upgrade had moderate cost. The BM31 phase 2 project however had a total investment budget of ~2 Million Euro's. Where 2021 was very much a development and investment year. 2022 was marked by a massive assembly, testing, installation and implementation works on especially the BM31 beamline while running practically a full user program. On BM31, 2023 has been devoted to, on the one hand, help the user community in making use of the new capabilities. While on the other hand, the sample environment for both stations was developed intensively in order to match with the new opportunities. On both beamlines much effort has also been put in streamlining the operation by further developing and implementing new software tools. All upgrades and development have been committed in the earlier years already anticipating the use of 2024 funds. As SNBL is running on a lean budget this meant that further developments in 2024 were put on hold in favor of ensuring the operations.

1. The user program was successfully and reliably executed on both beamlines.
2. 87 publications using SNBL data appeared in peer review journals, 38% of SNBL publications has an impact factor above 10 and 56% above impact factor 7.

The 2024 report provides a view on how SNBL positively impacts: 1) its partner country user community with experimental opportunities and education, 2) the larger synchrotron community with tools and fundamentals, 3) the ESRF user program and 4) European industry. SNBL provides a competitive edge to all its national users with its unique tools and expertise while at the same time also serving the whole synchrotron community with (software) tools and fundamental knowledge advancing science overall. As last year with the Bragg price, several early career scientists, working in both Norway and Switzerland have received international recognition through prizes, both heavily relying on SNBL. One of them started his synchrotron career at SNBL and is now a valued scientist at SLS2.

SNBL was reviewed by in 2024 by an international expert panel, the panel underpins the enormous impact it has on its user community and underlines the groundbreaking and leading role it has in synchrotron-based Energy and Catalysis research in Europe and beyond.

ESRF HIGHLIGHTS 2024



X-ray diffraction sheds light on CO₂-activated breathing-caloric materials for efficient refrigeration

This study combines variable-temperature and variable-pressure differential scanning calorimetry, and synchrotron powder X-ray diffraction to investigate large thermal changes in material MOF-508b, identifying it as a promising solid-state refrigerant for low-emission heating and cooling applications. A proof-of-concept thermometry device is also introduced.

The development of advanced thermomaterials for heating, ventilation, air-conditioning, and refrigeration (HVAC&R) has become a major focus, as this sector accounts for over 50% of global energy consumption and contributes approximately 50% of worldwide carbon emissions. In support of this energy transition, the European Union has enacted policies such as the Energy Efficiency Directive (EU-2023/955) and the F-gas Regulation (EU 2014/517), which aim to phase out fuel-burning heaters and high-global warming potential (GWP) refrigerant gases.

As a response, the HVAC&R industry has increasingly adopted CO₂ vapour-compression technologies. CO₂, commercially known as R-744, is widely available, non-toxic, non-flammable, and exhibits a much lower GWP than traditional refrigerants, facilitating a more circular carbon economy. However, CO₂-based HVAC&R systems require high operating pressures (70-150 bar) and have limited efficiency in warm climates above 31°C due to CO₂'s critical temperature, posing operational challenges.

An alternative approach is the development of solid-state thermomaterials that exhibit significant thermal responses under pressure-induced solid-solid phase transitions, known as barocaloric effects. These materials, however, are limited by high operational pressures (often exceeding 1000 bar) and relatively low thermal outputs compared to conventional refrigerants.

To address this, research has increasingly focused on metal-organic frameworks (MOFs), which undergo pressure-induced phase transitions. Specifically, certain MOFs exhibit reversible structural transitions between closed-pore and open-pore phases in response to gas pressurization, known as breathing transitions. Traditionally, MOFs with breathing transitions were primarily explored for gas adsorption, separation, and storage [1]. While these studies noted associated thermal changes, these were often considered undesirable for adsorption applications, leading to efforts aimed at minimizing these effects.

Recent work has aimed to identify MOFs that can maximize pressure-induced thermal changes for new eco-friendly refrigeration and heating technologies [2,3]. Specifically, this study focuses on MOF-508b ([Zn₂(bdc)₂(bpy)]), where bdc = 1,4-benzenedicarboxylate and bpy = 4,4'-bipyridine [3], which exhibits significant thermal changes when pressurized with CO₂. MOF-508b has three distinct polymorphs under varying CO₂ pressures, consisting of two interpenetrated 3D networks of Zn paddle-wheels linked by bdc ligands, with bpy pillars forming a hexagonal cavity structure (Figure 1a) [4]. Upon pressurization with CO₂, a shift in the subnetworks positions opens these cavities, facilitating CO₂ access.

These experiments employed variable-temperature and variable-pressure differential scanning calorimetry and synchrotron powder X-ray diffraction at beamline BM01 to explore the thermal behaviour of MOF-508b under CO₂ pressure (Figure 1b,c). Remarkably, thermal changes of $\Delta S \sim 460 \text{ J K}^{-1} \text{ kg}^{-1}$ were observed, outperforming many traditional refrigerants, including CO₂ alone. These thermal responses occur at pressures as low as 26 bar and extend the operational temperature range to 60°C – far exceeding CO₂'s critical temperature of 31°C.

Additionally, synchrotron powder X-ray diffraction enables correlation of these thermal effects with two distinct, pressure-induced solid-solid phase transitions (Figure 1c). These transitions are characterized by

minimal volume change compared to other MOFs, such as MIL-53(Al), which could reduce mechanical stresses in future HVAC&R devices.

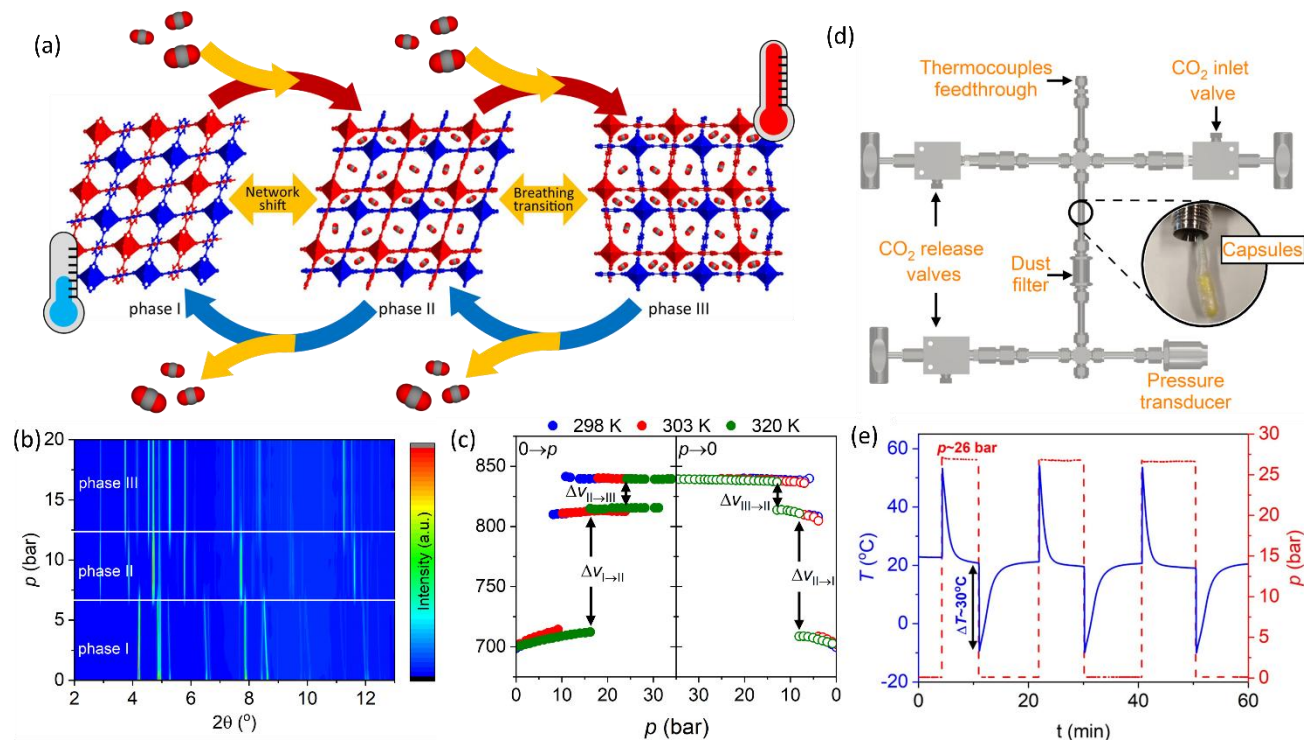


Fig. 1: **a)** Schematic of breathing-like transitions in MOF-508b. **b)** Evolution of synchrotron powder X-ray diffraction patterns at 298 K and **(c)** of volume changes for MOF-508b upon CO_2 pressurization at varying isothermal conditions. **d)** Schematic illustration of proof-of-concept thermometry device. **e)** Adiabatic temperature change observed in MOF-508b upon CO_2 pressurization/depressurization

The observed thermal changes in MOF-508b result from a combination of barocaloric effects (from the solid-solid phase transition) and CO_2 adsorption/desorption processes within the MOF-508b's pore structure – a novel cooling and heating mechanism referred to as “breathing-caloric effect”, in analogy to barocaloric, magnetocaloric, electrocaloric, and elastocaloric effects [5].

A prototype, proof-of-concept thermometry device developed in this study (Figure 1d) demonstrated that MOF-508b exhibits adiabatic temperature changes of up to 30 K under 26 bar of CO_2 pressure. At ambient conditions, MOF-508b can reach temperatures as high as 58°C or as low as -10°C, depending on CO_2 pressurization and depressurization cycles within a range of 1-26 bar (Figure 1e).

These findings underscore the potential of breathing-caloric materials like MOF-508b for innovative applications in HVAC&R. With their substantial thermal shifts and relatively low operating pressures, these materials offer a viable path toward energy-efficient, eco-friendly heat-pumps and refrigeration technologies, potentially achieving even sub-zero temperatures. This research represents a step forward in sustainable thermal management solutions, aligning with global energy transition goals.

Principal publication and authors

Empowering CO₂ Eco-Refrigeration With Colossal Breathing-Caloric-Like Effects in MOF-508b, M. Gelpi (a), J. García-Ben (a), S. Rodríguez-Hermida (b), J. López-Beceiro (c), R. Artiaga (c), Á. Baaliña (d), M. Romero-Gómez (d), J. Romero-Gómez (d), S. Zaragoza (c), J. Salgado-Beceiro (e), J. Walker (f), C.J. McMonagle (G), S. Castro-García (a), M. Sánchez-Andújar(a), M.A. Señarís-Rodríguez (a), J.M. Bermúdez-García (a), *Adv. Mater.* 36, 10499 (2024); <https://doi.org/10.1002/adma.202310499>

(a) QuiMolMat Group, Department of Chemistry, Faculty of Science and Centro Interdisciplinar de Química e Bioloxía (CICA), University of A Coruña, Zapateira (Spain)

(b) Research Support Services, University of A Coruña, A Coruña (Spain)

(c) CITENI-Proterm Group, Ferrol Industrial Campus, Campus de Esteiro, University of A Coruña, Ferrol (Spain)

(d) Energy Engineering Research Group, Department of Nautical Sciences and Marine Engineering (ETSNM), University Institute of Maritime Studies, University of A Coruña, A Coruña (Spain)

(e) SINTEF Energy Research, Trondheim (Norway)

(f) Department of Materials Science and Engineering, Norwegian University of Science and Technology, Trondheim (Norway)

(g) Swiss-Norwegian beamlines, ESRF

References

[1] K. Barthelet *et al.*, *Angew. Chem. Int. Ed.* 41, 281-284 (2002).

[2] J. García-Ben *et al.*, *Chem. Mater.* 34, 3323-3332 (2022).

[3] M. Gelpi *et al.*, *Adv. Mater.* 2310499, 1-9 (2023).

[4] P.M. Bhatt *et al.*, *Chem. Commun.* 52, 11374-11377 (2016).

[5] S. Fähler *et al.*, *Adv. Eng. Mater.* 14, 10-19 (2012).



Norwegian University of
Science and Technology



Operando X-ray spectroscopy reveals insights into the stability of novel catalysts for CO₂ reduction

One of the primary challenges in advancing the technological implementation of electrochemical CO₂ conversion is ensuring the long-term stability of the catalysts used. *Operando* X-ray spectroscopy experiments offer crucial insights into the design of catalysts that remain structurally stable over time.

Developing catalysts that are active, selective and stable is one of the most significant challenges to overcome in the pursuit of a more sustainable society. There is an urgent need to improve the stability of electrocatalysts that facilitate CO₂ utilization through the production of valuable chemicals. Among potential catalysts, copper stands out as the most promising for generating products beyond CO – such as methane, ethylene, and ethanol – via the electrochemical CO₂ reduction reaction (CO₂RR). However, copper undergoes drastic and unpredictable structural reconstruction, leading to performance losses and obscuring the inherent sensitivities of the reaction to the catalyst's geometric structure.

This study introduces a novel material solution to address the challenge of catalyst stability in CO₂RR. In particular, it demonstrates that a hybrid organic/inorganic coating can stabilize copper electrocatalysts, preventing structural reconstruction.

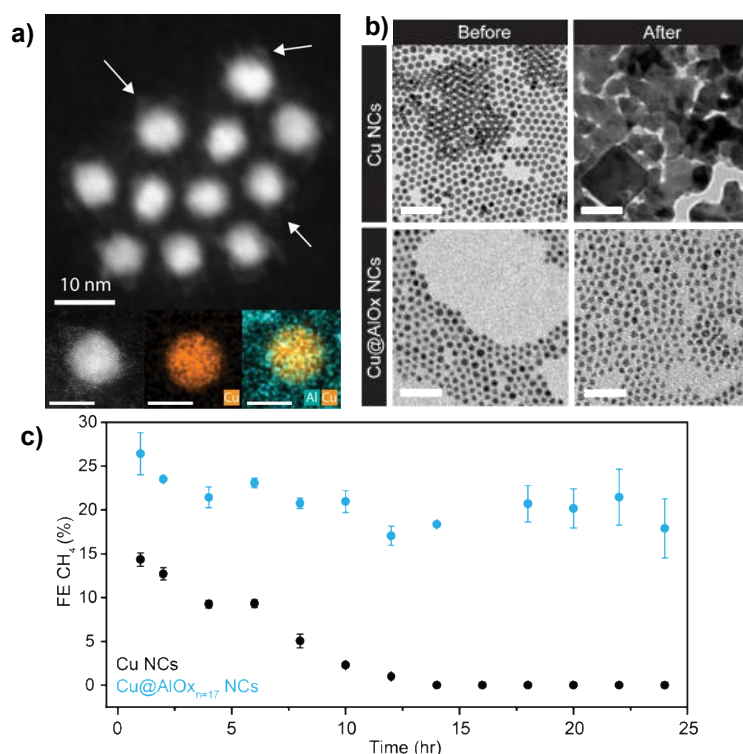


Fig. 1: a) Representative scanning transmission microscopy image of Cu@AlOx NCs, with white arrows pointing at the amorphous alumina coating surrounding the metallic Cu NC core, along with elemental mapping at the single particle level; b) Representative electron microscopy images of Cu NCs and Cu@AlOx NCs before and after 4 h CO₂RR at -1.1 V versus RHE. Scale bars, 50 nm; c) Temporal evolution of the faradaic efficiency for methane for as-synthesized Cu NCs and Cu@AlOx_{n=17} NCs at -1.1 V versus RHE. The data are the average of six measurements (every 2 h), and the error bars are the calculated standard deviation.

The materials developed in this research consist of copper nanocrystals (NCs) encased in a hybrid AlOx shell with adjustable thickness, which incorporates organic ligands (Figure 1a). These materials are referred to as Cu@AlOx NCs. The Cu NCs are synthesized using colloidal chemistry, while the hybrid AlOx shell is prepared

through a recently developed method known as colloidal atomic layer deposition (c-ALD). This approach simulates the gas-phase deposition process in an aprotic solvent. The Cu@AlOx NCs exhibit superior structural stability compared to uncoated Cu NCs (Figure 1b), resulting in more stable methane production during CO₂RR (Figure 1c).

In addition to various other techniques and control experiments, *operando* X-ray absorption spectroscopy studies were performed at beamline BM31. X-ray absorption near-edge structure (XANES) data collected at the Cu K-edge revealed a mixture of copper species (Cu⁰, Cu⁺, Cu²⁺) at open circuit potential (OCP) for both samples (Figure 2a,b). However, notable differences emerged between the samples during CO₂RR. Specifically, the Cu@AlOx retained a significant fraction of Cu²⁺ during operation, whereas the Cu NCs existed primarily in their metallic state (Figure 2a,b). To corroborate the trends observed in XANES, *operando* extended X-ray absorption fine structure (EXAFS) spectroscopy indicated the retention of a Cu-O(Al) feature, suggesting the persistence of interaction between oxidized copper and the alumina network (Figure 2c). This data enables the construction of an atomistic picture of the Cu|AlOx interface and the structure of the active sites (Figure 2d).

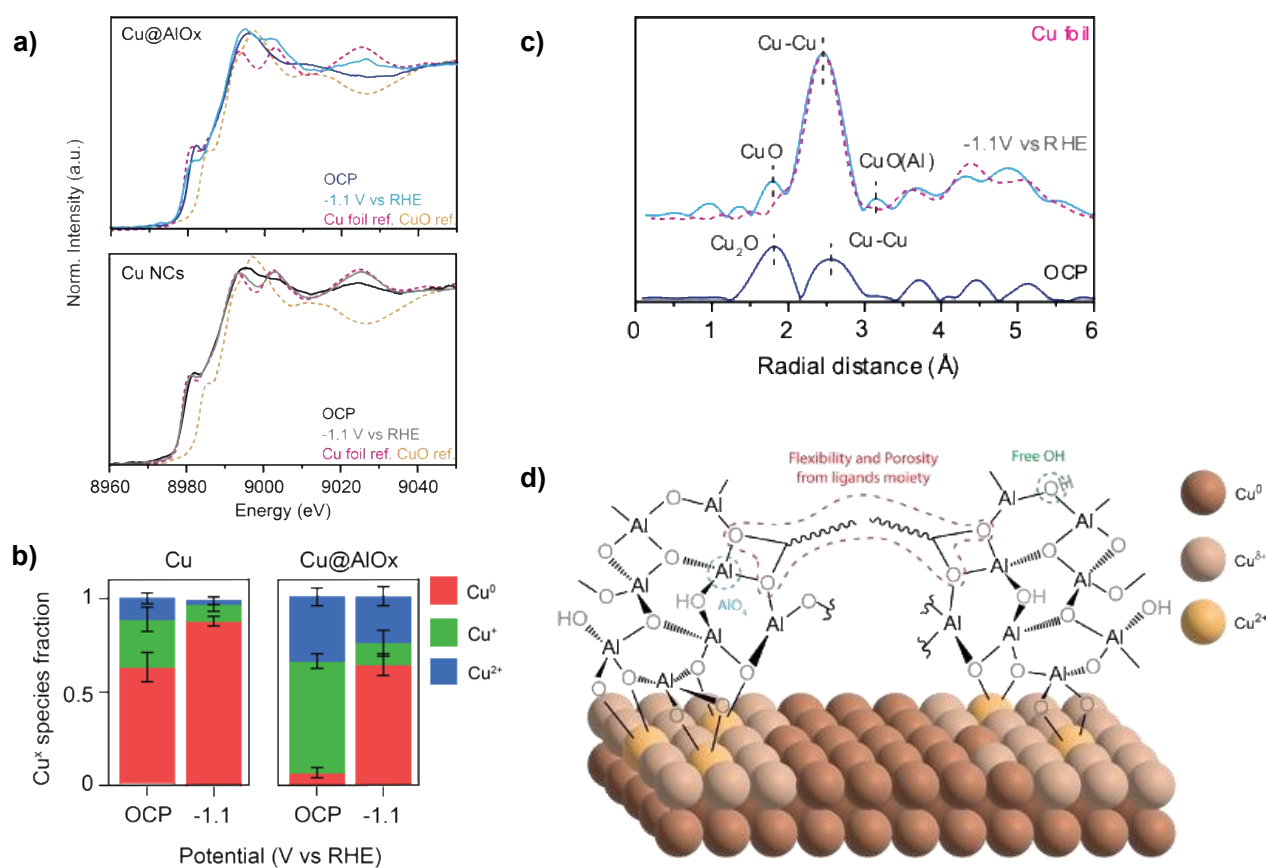


Fig. 2: **a)** Cu K-edge XANES spectra of Cu NCs and Cu@AlOx NCs at OCP and at -1.1 V versus RHE during CO₂RR; **b)** Cu^x species fraction at OCP and at -1.1 V versus RHE during CO₂RR extracted from a); **c)** EXAFS data of Cu@AlOx NCs at OCP and at -1.1 V versus RHE during CO₂RR; **d)** Schematic representation of the interface in the Cu@AlOx electrocatalysts with the key chemical and structural features

Current understanding highlights that redox processes, and the subsequent dissolution and reprecipitation of transient, soluble Cu intermediate species, are the primary drivers of copper reconstruction during both the start-up and shut-down of the electrochemical cell and during CO₂RR itself [1,2]. The AlOx coating effectively stabilizes the oxidation state of a significant portion of the copper surface, making it less susceptible to the

redox processes responsible for copper reconstruction. Concomitantly, the AlO_x coating contributes to locally confine atomic diffusion, which further contributes to limit the copper restructuring.

It was also discovered that the intrinsic activity of the Cu atoms in the Cu@AlO_x catalysts doubles compared to that of the uncoated Cu NCs, which results from the electronic interactions between the copper and the oxide coating. Furthermore, the conversion of CO₂ can be steered towards the production of ethylene by changing the reaction medium, specifically the cation in the electrolyte. This result is important because it highlights the versatility of this catalytic system.

In conclusion, this work presents a strategic approach to designing stable electrocatalysts for CO₂ conversion. As the chemistry is general, the principles demonstrated here can be extended to other materials and reactions in the future.

Principal publication and authors

Hybrid oxide coatings generate stable Cu catalysts for CO₂ electrolysis, P.P. Albertini (a), M.A. Newton (a), M. Wang (a), O.S. Lecina (a), P.B. Green (a), D.C. Stoian (b), E. Oveisi (c), A. Loiudice (a), R. Buonsanti (a), *Nat. Mater.* 23, 680-687 (2024); <https://doi.org/10.1038/s41563-024-01819-x>

(a) *Laboratory of Nanochemistry for Energy (LNCE), Institute of Chemical Sciences and Engineering (ISIC), École Polytechnique Fédérale de Lausanne (Switzerland)*

(b) *Swiss-Norwegian Beamlines, ESRF*

(c) *Interdisciplinary Center for Electron Microscopy (CIME), École Polytechnique Fédérale de Lausanne (Switzerland)*

References

[1] J. Vavra *et al.*, *Nat. Catal.* 7, 89-97 (2024).

[2] J. Vavra *et al.*, *Angew. Chemie. Int. Ed.* 60, 1347-1354 (2021)

The logo of EPFL (École Polytechnique Fédérale de Lausanne) is displayed in a bold, red, sans-serif font. The letters are stylized, with the 'E' and 'F' having a distinctive blocky appearance.

Operando X-ray analysis of nickel gallium catalysts for CO₂ hydrogenation to methanol

Operando X-ray absorption and X-ray total scattering techniques were used to study Ni_xGa_(100-x)/SiO₂ catalysts for CO₂ hydrogenation to methanol, a promising technology for advancing carbon neutrality in the chemical industry. The analysis revealed that a nickel gallium (Ni-Ga) alloy, along with small amounts of gallium oxides (GaO_x), promotes high methanol activity and selectivity. Optimizing the Ni:Ga ratio is key to enhancing catalytic performance.

The selective conversion of the greenhouse gas CO₂ into methanol is a key step toward a more carbon-neutral chemical industry. Developing efficient catalysts that offer high CO₂ conversion and methanol selectivity, while minimizing the formation of side products such as CO or CH₄, is essential. In this context, progress in catalyst development relies on understanding the structure of the active sites.

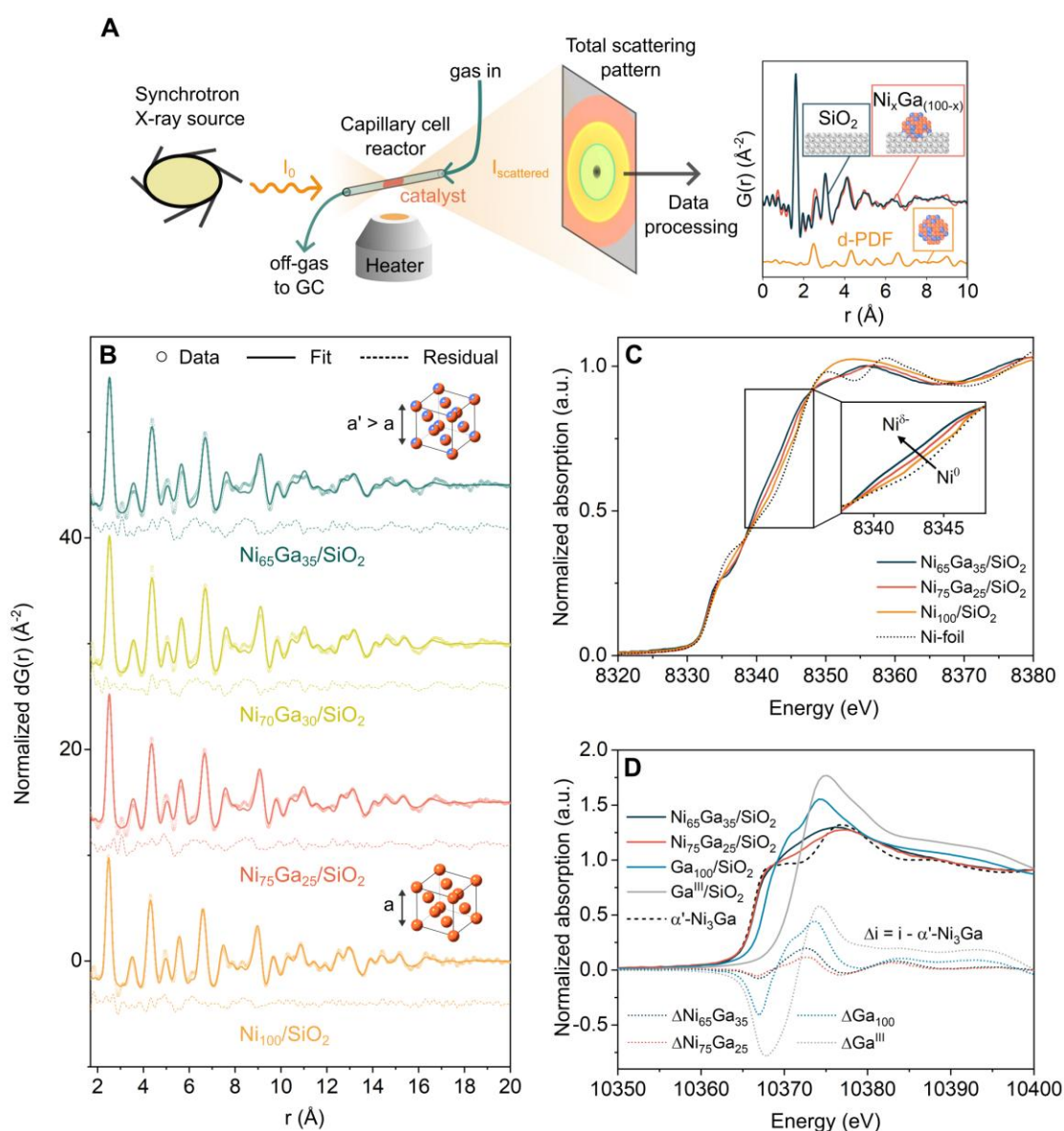


Fig. 1: **a)** Schematic of the X-ray total scattering experiment and the corresponding d-PDF analysis. **b)** d-PDF data fitted to an fcc Ni-Ga alloy structure. **c)** Normalized Ni K-edge XANES spectra of Ni_xGa_(100-x)/SiO₂ compared to Ni-foil. **d)** Normalized Ga K-edge XANES and difference XANES spectra of Ni_xGa_(100-x)/SiO₂ compared to α'-Ni₃Ga and Ga^{III}/SiO₂ reference materials.

Nickel-based catalysts are well known for their high activity in CO₂ hydrogenation to CH₄. Interestingly, when nickel is alloyed with gallium in an intermetallic phase, methane formation is suppressed, and the selectivity shifts towards methanol [1]. However, elucidating the structural features (both electronic and geometric) responsible for this shift in selectivity in Ni-Ga-based catalysts has been challenging due to a lack of model catalyst systems with precise control over particle size, phase, and composition (i.e., the Ni:Ga ratio) and the difficulty of probing these structural features under catalytically relevant conditions.

To address these challenges, a series of silica-supported Ni-Ga-based catalysts with varying Ni:Ga ratios (Ni_xGa_(100-x)/SiO₂) was prepared via a surface organometallic chemistry approach [2], allowing for precise control over the metal loading. This method yielded Ni-Ga nanoparticles with different Ni-Ga ratios but uniform particle size (ca. 2 nm). The structure of the catalysts was probed using *operando* X-ray absorption spectroscopy (XAS) at the Ni and Ga K edges (acquisition time ca. 3 minutes per scan) at beamline BM31 and X-ray total scattering at beamline ID15A (acquisition time ca. 5 minutes per scan). The catalysts were characterized both after *in-situ* activation in H₂ at 600°C and under CO₂ hydrogenation conditions at 230°C and 20 bar (using a CO₂:H₂:N₂ gas mixture in a ratio of 1:3:1). These experiments were conducted in a capillary cell reactor with online off-gas analysis via gas chromatography. Additionally, differential pair distribution function analysis (d-PDF) of the X-ray total scattering data was performed, subtracting the scattering contribution from the amorphous SiO₂ support from the total scattering pattern of the Ni_xGa_(100-x)/SiO₂ (Figure 1a).

Modelling of the d-PDF revealed a face-centred cubic (fcc) Ni-Ga random alloy for all catalyst compositions (Figure 1b). Based on Vegard's law, the Ga content in the Ni-Ga alloy was determined and found to be lower than the nominal Ni:Ga ratio determined by ICP-OES, indicating that some Ga was not incorporated into the fcc structure. Ga K-edge XAS experiments further revealed that the unincorporated Ga existed as GaO_x (Figure 1d).

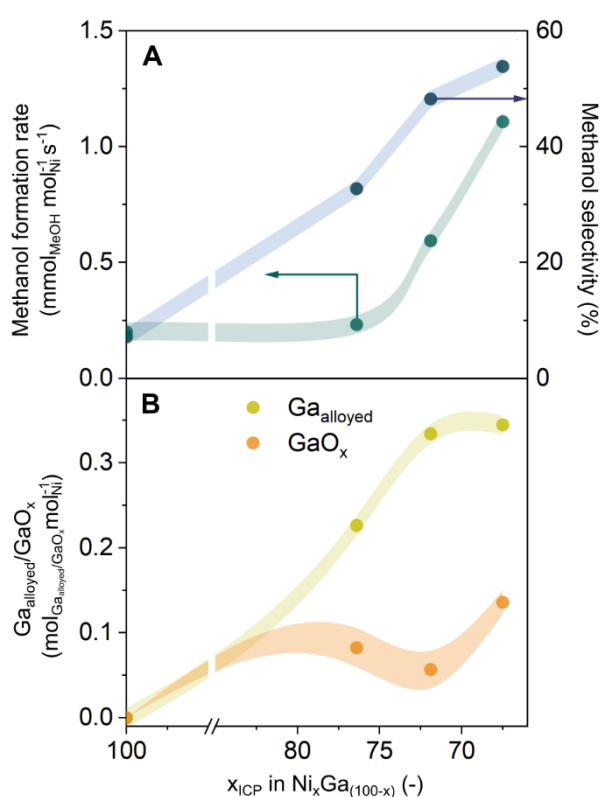


Fig. 2: **a)** Methanol formation rate and methanol selectivity (averaged over the first 180 minutes) as a function of the catalyst composition, determined by elemental analysis and denoted as x_{ICP} in Ni_xGa_(100-x)/SiO₂. **b)** Ga_{alloyed} and GaO_x contents as a function of x_{ICP} . Shaded lines serve as visual guides.

Combining the structural and performance data (Figure 2), several key observations were made: (i) the presence of an fcc Ni-Ga alloy is crucial for achieving high methanol selectivity; (ii) small quantities of GaO_x in addition to the Ni-Ga alloy promote methanol formation, as evidenced by comparing two catalysts with similar Ni:Ga ratios in the alloy but differing GaO_x content; (iii) the catalyst with the highest methanol selectivity (Ni₆₅Ga₃₅/SiO₂) contained the most Ga-rich fcc alloy with a Ni:Ga molar ratio of approximately 3:1, along with a minor quantity of oxidized Ga species.

Additional Ni K-edge XAS experiments revealed that (i) Ni was fully metallic in all catalysts studied, and (ii) alloying Ni with Ga modified the electronic structure of Ni, forming Ni^{δ-} species (Figure 1c). Tracking the structure of the most active Ni₆₅Ga₃₅/SiO₂ catalyst under CO₂ hydrogenation conditions over ~ 4 hours of time on stream showed that the Ni-Ga alloy nanoparticles retained their structure and composition, with no evidence of dealloying or further alloying, correlating with a stable methanol production rate. Complementary *operando* DRIFTS experiments suggested that GaO_x species facilitate CO₂ activation and stabilize formate species on the catalyst surface, which are reaction intermediates in CO₂ hydrogenation to methanol.

These findings offer fundamental insights into the reactivity of Ni-Ga-based catalysts and provide guidelines for further enhancing catalytic performance. The combination of *operando* X-ray scattering, XAS, and DRIFTS enables the formulation of quantitative structure-performance relationships. Overall, optimizing both the Ni:Ga ratio in the alloy and the quantity of GaO_x species is key to obtaining catalysts with high methanol selectivity and production rates.

Principal publication and authors

Structure and Role of a Ga-Promoter in Ni-Based Catalysts for the Selective Hydrogenation of CO₂ to Methanol, N. K. Zimmerli (a), L. Rochlitz (b), S. Checchia (c), C.R. Müller (a), C. Copéret (b), P.M. Abdala (a), *JACS Au* **4** (1), 237-252 (2024); <https://doi.org/10.1021/jacsau.3c00677>

(a) Department of Mechanical and Process Engineering, ETH Zürich, Zürich (Switzerland)

(b) Department of Chemistry and Applied Biosciences, ETH Zürich, Zürich (Switzerland)

(c) ESRF

References

[1] F. Studt *et al.*, *Nat Chem.* **6**, 320-324 (2014).

[2] C. Copéret, *Acc. Chem. Res.* **52**, 1697-1708 (2019).

The logo for ETH Zürich, featuring the letters 'ETH' in a bold, black, sans-serif font, followed by 'zürich' in a lowercase, black, sans-serif font with a lowercase 'z'.

X-ray spectroscopy reveals particle size-dependent selectivity in cobalt CO₂ hydrogenation catalysts

Researchers from BP and ETH Zürich in Switzerland examined how cobalt nanoparticle size influences CO₂ hydrogenation, a key reaction in sustainable fuel production. Operando X-ray spectroscopy reveals that smaller particles (1.6 nm) oxidize fully and favour the reverse water-gas shift (RWGS) reaction, producing CO, while larger particles (2.1–3.0 nm) stay metallic, enhancing methanation.

This work investigated particle size dependence in cobalt-based CO₂ hydrogenation, an important catalytic reaction contributing to a closed-carbon cycle through sustainable fuels and chemical synthesis. Using surface organometallic chemistry (SOMC), a series of silica-supported cobalt nanoparticles ranging from 1.6 to 3.0 nm were synthesized and their catalytic performance evaluated under CO₂ hydrogenation conditions. The results reveal a strong dependence of catalytic behaviour on particle size: very small particles (1.6 nm) favour the reverse water-gas shift (RWGS) reaction, producing CO as the primary product, while larger particles (2.1 and 3.0 nm) tend toward methanation, as expected for cobalt catalysts in CO₂ hydrogenation.

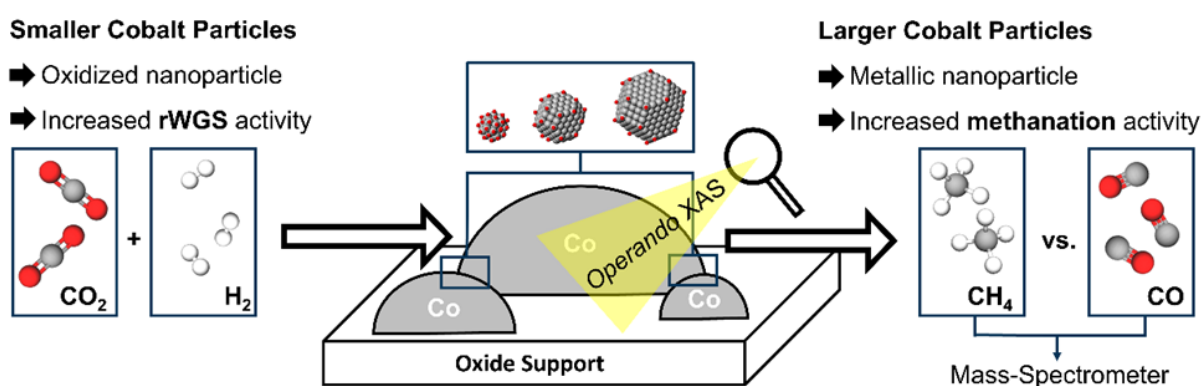


Fig. 1: Schematic summary of particle size effect in cobalt-based CO₂ hydrogenation, linking particle size, propensity of cobalt to be oxidized, and product selectivity.

Operando X-ray absorption spectroscopy (XAS) experiments performed at the Swiss Norwegian Beamline (SNBL) BM31 demonstrated that differences in catalytic selectivity are strongly linked to the oxidation state of cobalt particles during reaction conditions. Smaller cobalt nanoparticles undergo complete oxidation, which shifts their reactivity to predominantly RWGS. In contrast, larger particles (> 2.0 nm) maintain a metallic state, favouring methane production due to enhanced oxidation resistance. These findings provide insight into tuning the selectivity of cobalt-based CO₂ hydrogenation catalysts, highlighting the importance of cobalt's oxidation state in determining catalytic outcomes, with small particles specifically promoting RWGS.

Principal publication and authors

Small Cobalt Nanoparticles Favor Reverse Water-Gas Shift Reaction Over Methanation Under CO₂ Hydrogenation Conditions, Xiaoyu Zhou (a), Dr. Gregory A. Price (b), Dr. Glenn J. Sunley (b), Prof. Dr. Christophe Copéret (a), *Angew. Chem.* 62(52) e202314274 (2023); <https://doi.org/10.1002/anie.202314274>

(a) Department of Chemistry and Applied Biosciences, ETH Zürich, Zürich (Switzerland)

(b) BP Innovation & Engineering, Applied Sciences, BP plc, Saltend, Hull (UK)

Research results from users enabled by the BM31 upgrade

The BM31 upgrade was completed only very recently, in the summer of 2022, and many of the results from novel advanced experiments are still being processed. Nonetheless, the following two 2024 papers highlight some of the unique new capabilities of BM31. In the first example, a combined dual edge XAS-PDF experiment was performed on a charging and discharging battery. As for the second example, the experiment itself was relatively basic, ex-situ XAS-PDF, the data on the other hand was used for very advanced modeling with RMC-Profile. RMC-Profile can fit many data types simultaneously (Neutron & X-ray total scattering & the Bragg profile, EXAFS, single crystal diffuse scattering) and produce atomic models that are consistent with all the available data. In this case reverse Monte-Carlo simulations produced models of full nanoparticles during different stages of a synthesis process. The developers of RMC-Profile have shown interest in using the combined datasets from BM31.

(De)sodiation Mechanism of Bi_2MoO_6 in Na-Ion Batteries Probed by Quasi-Simultaneous Operando PDF and XAS

Sodium ion batteries are researched for the potential use in ground-based applications large storage facilities, due to the larger mass, but much lower cost of sodium compared with lithium. Cathodes may use the intercalation mechanism typical in Li-ion batteries, but a conversion alloy mechanism is also often employed. In this paper Bi_2MoO_6 is investigated. The Bi and Mo edges and PDF data were taken continuously during charge and discharge. The oxide quickly decomposes into Bi metal nanoparticles and the remaining binary oxide, which is typical of bismuth metal oxide cathodes. The Bi then alloys with the Na during discharge. XRD showed the change over 1.5 cycles $\text{Bi}_2\text{MoO}_6 \rightarrow \text{Bi} \leftrightarrow \text{NaBi} \leftrightarrow \text{c-Na}_3\text{Bi}$. Bi XANES showed a reduction from +3 to 0 at the beginning of the first sodiation, then from 0 to -3 at the end of sodiation. In later cycles, the Bi oxidation state reached above 0, but $< +3$ at the end of desodiation (not fully returning to its original state as in the oxide). See Figure 1

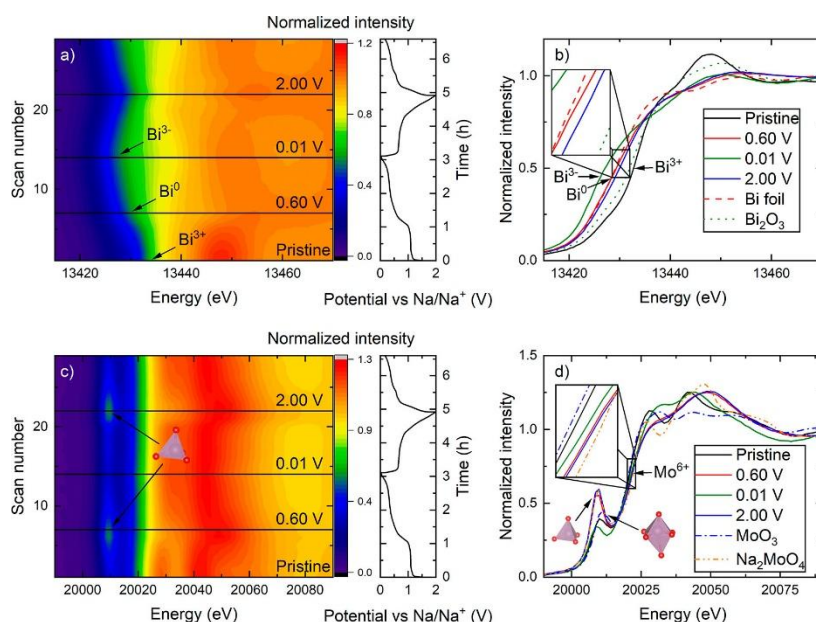


Figure 1 Contour plots obtained from operando XANES measurement of (a) Bi L3 edge and (c) Mo K edge, including corresponding (de)sodiation curves obtained from GC at 0.2 A g^{-1} and $0.01\text{--}2.00 \text{ V}$ vs Na/Na^+ . Selected scans of (b) Bi L3 edge and (d) Mo K edge vs references with zoomed in insets to highlight the differences in edge position. The black lines in (a,c) correspond to the XANES graphs shown in (b,d).

The fraction of Bi^{3+} at the end of desodiation decreased over cycle number. Fourier transformed EXAFS data corroborates this, as the intensity of the Bi-O peak decreases over cycle number as well, while the Bi-Bi intensity increases slightly. The Mo oxidation state remains close to +6 throughout cycling. Mo geometry changes from distorted octahedral to tetrahedral, judging from the increase in intensity of the pre-edge feature Mo-O peak in EXAFS FT becomes sharper and shifts to shorter distance, also indicating change to tetrahedral geometry.

In PDF an initial reduction in pair-correlation lengths indicate a reduction in coherent crystallite size and significant change in the short-range structure during the conversion of Bi_2MoO_6 to Bi metal. PDF and XRD then showed how the particle size of the BiNi alloys evolved over time – gradually increasing over cycle

number. This is one mechanism of degradation of the cells as it reduces the available surface area for Na absorption. See Figure 2.

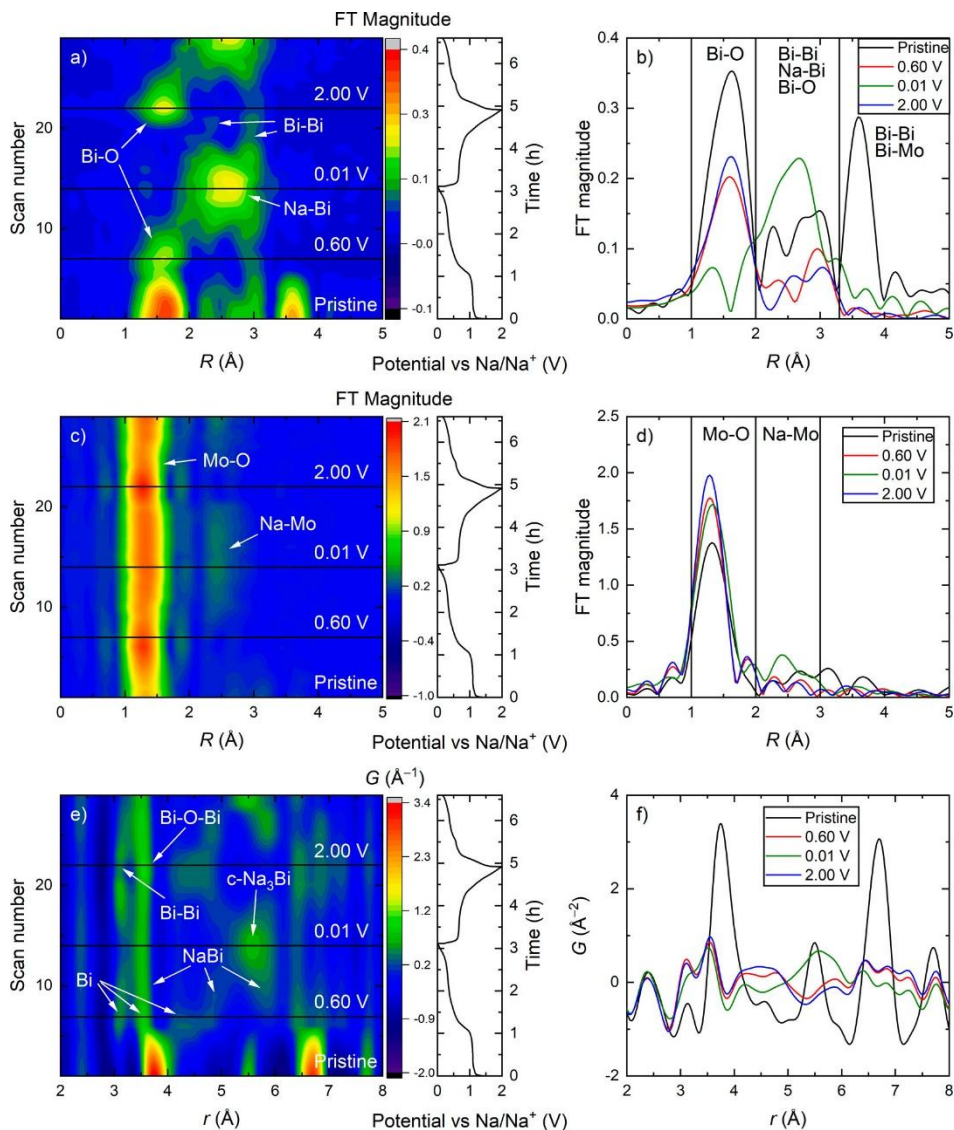


Figure 2 FT EXAFS contour plots of (a) Bi L3 and (c) Mo K, including (de)sodiation curves obtained by GC at 0.2 A g⁻¹ and 0.01–2.00 V vs Na/Na⁺. (e) PDF contour plot with labels highlighting the peaks corresponding to the closest Bi–Bi bonds in each of the Na_xBi phases. (b), (d,f) selected scans extracted from the plots in (a,c,e) marked with black lines.

The PDF and XAS provided complimentary data, with PDF giving information on particle size and local structure information, especially on Bi, while XAS gave information about the evolution of oxidation states, and local environments around Mo and Bi. EXAFS and PDF showed the disappearance of the Bi-O peaks over the course of several cycles.

Principal publication and authors

(De)sodiation Mechanism of Bi₂MoO₆ in Na-Ion Batteries Probed by Quasi-Simultaneous Operando PDF and XAS, A. Brennhagen (a), A. Skurtveit (a), D.S. Wragg (a,b), C. Cavallo (c), A.O. Sjøstad (a), A.Y. Kuposov (a,b), H. Fjellvåg (a), **Chemistry of Materials** (2024); 10.1021/acs.chemmater.4c01503

(a) Centre for Materials Science and Nanotechnology, Department of Chemistry, University of Oslo, Norway

(b) Department of Battery Technology, Institute for Energy Technology, Kjeller, Norway

(c) FAAM, Battery production, Italy



UiO : **University of Oslo**

IFE Institute for
Energy Technology

FAAM
Energy Saving Battery

Nucleation-Mediated Structure Selection Kinetics of Self-assembled Cobalt Nanoparticles in Solution and Catalytic State Formation

Cobalt oxide, oxyhydroxide and Co_3BO_x nanoparticles were synthesized from $\text{Co}(\text{NO}_3)_2$ and BF solutions under different conditions: under LED illumination or not, and with or without the addition of a combined Ru complex salt and $\text{Na}_2\text{S}_2\text{O}_8$, which together with the Co compounds form an oxygen evolution catalyst. The Co gradually oxidizes during the reaction forming Co_3O_4 then CoOOH (Table 1).

Table 1. Synthetic parameters used for the synthesis of Co-NPs

Condition	Reaction time	$\text{Na}_2\text{S}_2\text{O}_8$ (mM)	$[\text{Ru}(\text{bpy})_3]^{2+}$ (mM)	Sample ID
LED-(L) illumination	1 h	—	—	RL1h-NPs [†]
Photocatalytic LED-(L) illumination	1 min	5.0	1.0	L1m-NPs
	10 min	5.0	1.0	L10m-NPs
	1 h	5.0	1.0	L1h-NPs
	20 h	5.0	1.0	L20h-NPs
Dark (D)	1 min	5.0	1.0	D1m-NPs
	10 min	5.0	1.0	D10m-NPs
	1 h	5.0	1.0	D1h-NPs
	20 h	5.0	1.0	D20h-NPs

[†]Self-assembled RL1h-NPs were synthesized by stirring the mixture of only $\text{Co}(\text{NO}_3)_2$ (10 mM) in borate buffer (36 mL, 80 mM, pH 8.5, Methods).

Small differences in the resulting structures led to observable differences in the yield of oxygen evolution reactions. The products were characterized using PDF and XAS. PDF and XAS were modelled together using reverse Monte-Carlo with full nanoparticle models using RMCProfile. This was used to find the composition, size and degree of disorder in the nanoparticles by analyzing the range of bond angles compared with the ideal structure.

Aliquots of the reactions were taken periodically for measurement, which showed the evolution of particle synthesis. XANES on the control, in light, without the Na and Ru compounds, showed that the Co oxidation state was in between that of $\text{Co}_3\text{B}_2\text{O}_6$ (+2) and Co_3BO_5 (+2.3), at $\sim+2.09$ after 1 hour of reaction. This was similar to the sample synthesized in the dark, after 1 minute. The samples synthesized in the dark quickly formed Co_3O_4 (+8/3) and then CoOOH (+3) after some time. Under illumination the reaction is faster, with the borate phase not being observed.

The samples were tested for photocatalytic activity for oxygen evolution from water. The conditions for the reaction are similar to the synthesis of the 'L' samples, and so the nanoparticles continue to evolve during this process. However, they are long lived enough that it has a substantial impact on the O_2 yield (Table 2).

Table 2. Structure properties of the investigated Co-NPs as derived from the analysis of their $\text{FT}[k^3\chi(k)]$ spectra and $G(r)$ functions[‡]

Sample ID	Phase	Size (Å)	B-O (Å)	$N_{\text{B-O}}^{\dagger}$	Co-O (Å)	$N_{\text{Co-O}}$	CoO-CoO (Å)	$N_{\text{Co-Co}}$	CoO-CoO (Å)	$N_{\text{Co-Co}}$	Co-H [§] (Å)	$N_{\text{Co-H}}$	Valence state	O_2 yield ^f
RL1h-NPs	Co_3BO_x	38.5	1.49	2.98	2.076	5.94	3.119	5.92	—	—	—	—	2.09	65
L1m-NPs	Co_3O_4	27.5	—	—	1.948	5.18	2.849	5.92	3.387	11.94	—	—	2.54	12
L10m-NPs	CoOOH	40	—	—	1.914	5.94	2.842	5.94	—	—	2.718	5.92	2.72	43
L1h-NPs	CoOOH	40	—	—	1.906	5.94	2.843	5.94	—	—	2.683	5.92	2.79	82
L20h-NPs	CoOOH	60	—	—	1.918	5.94	2.848	5.94	—	—	2.716	5.92	2.88	34
D1m-NPs	Co_3BO_x	38.5	1.46	2.98	2.057	5.94	3.092	5.92	—	—	—	—	2.11	82
D10m-NPs	Co_3O_4	60	—	—	1.979	5.26	2.898	5.92	3.382	11.92	—	—	2.46	17
D1h-NPs	CoOOH	40	—	—	1.912	5.94	2.842	5.94	—	—	2.683	5.92	2.76	63
D20h-NPs	CoOOH	60	—	—	1.915	5.94	2.851	5.94	—	—	2.721	5.92	2.83	48

[‡]The tabulated interatomic distances and coordination numbers ($N_{i,j}$) are the average values over those obtained from analysis of the $\text{FT}[k^3\chi(k)]$ spectra and $G(r)$ functions, and include the contribution from undercoordinated $\{\text{CoO}_x\}$ and $\{\text{BO}_x\}$ units arising on the surface of the different Co-NPs.

[†] $N_{\text{B-O}}$, $N_{\text{Co-O}}$, $N_{\text{Co-Co}}$ and $N_{\text{Co-H}}$ denote the main coordination number of the corresponding B-O, Co-O, Co-Co and Co-H pair-atoms.

[§]The notation Co-H indicates the interatomic distance between Co and H pairs-atoms in the CoOOH structure, not a hydride bond.

^fThe O_2 yield of RL1h-NPs corresponds to the first OER cycle. The O_2 yield of all other Co-NPs corresponds to the second OER cycle.

DFT was used to investigate the oxygen evolution reaction on the surface of Co oxyborite. 5 possible pathways were identified, including on Co and B sites.

Here PDF and EXAFS together were used to provide a model of the entire nanoparticles, Figure 1. The results of the RMC refinements were then used in DFT to provide information about catalytic mechanisms. XANES was used to find the oxidation states, and so also gave information about where the material was on the reaction coordinate between $\text{Co}_3\text{B}_2\text{O}_6$ and Co_3BO_5 , and then between Co_3O_4 and COOH .

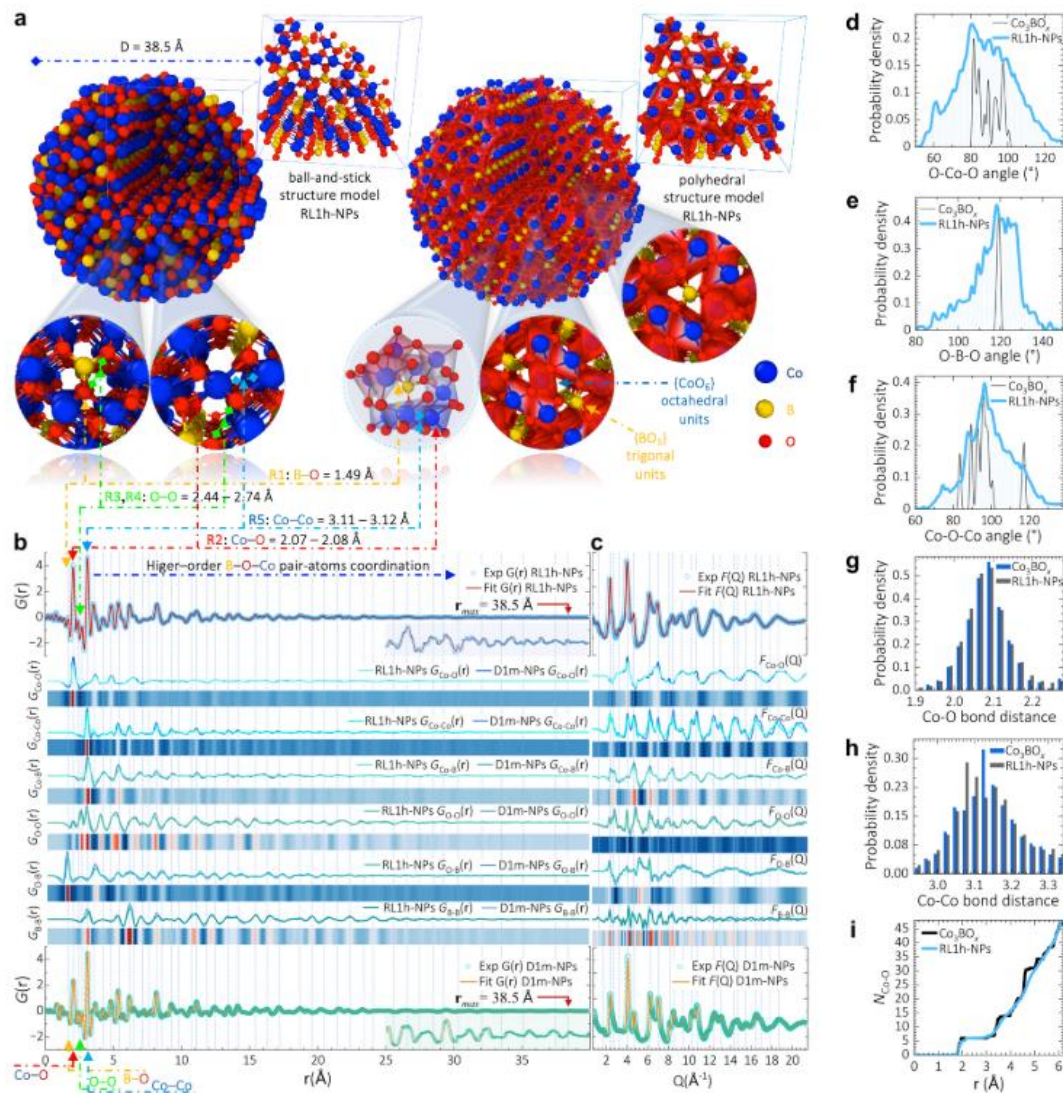


Figure 1, Modeling of the intermediate-range order of RL1h- and D1m-NPs. **a**, RMC simulated structure of RL1h-NP. **b,c**, RMC fitting of $F(Q)$ and $G(r)$ functions of RL1h-NPs (top) and D1m-NPs (bottom), and the insets zoom the 25-40 Å region. Distribution of Co-O and B-O bond-distances and high-order pair-atoms interatomic distances are given by the partial $G_{\text{Co-O}}(r)$, $G_{\text{B-O}}(r)$, $G_{\text{Co-Co}}(r)$, $G_{\text{B-B}}(r)$, $G_{\text{O-O}}(r)$ signals. The contributions of the different pair-atoms to the $F(Q)$ functions are given by the partial $F_{\text{Co-O}}(Q)$, $F_{\text{B-O}}(Q)$, $F_{\text{Co-Co}}(Q)$, $F_{\text{B-B}}(Q)$, $F_{\text{O-O}}(Q)$ signals, **d-i**, Distributions of bond-angles, bond-distances and atomic coordination RL1h-NP and crystalline Co_3BO_5

Principal preprint and authors

Structure-Selection Dynamics of Cobalt Nanoparticles from Solution Synthesis and Their Impact on the Oxygen Evolution Reaction

Greta R. Patzke (a), Florian Keller (a), Marcella Iannuzzi (a), Lukas Reith (a), Kenneth Paul Marshall (b), Wouter van Beek (b), and Carlos A. Triana (a) *ACS Nano* **2024** *18* (52), 35533-35549

(a) Department of Chemistry, University of Zurich, Zurich, Switzerland

(b) The Swiss-Norwegian Beamlines (SNBL), European Synchrotron Radiation Facility (ESRF), France



**Universität
Zürich^{UZH}**

SNBL's staff research impacting the larger synchrotron community

Development of theoretical aspects of modern synchrotron diffraction geometries.

This scientific program is mostly initiated by SNBL staff, with an active participation of various user groups. The highlighted research concerns a theoretical analysis of instrumental contribution in the width of diffraction lines for diffractometry with large 2D detectors (Chernyshov et al., 2021), and its appearance in PDF patterns is developed (Chernyshov et al., 2024). This work has a wide impact on the larger (synchrotron) diffraction community as traditional instrumental shape models have serious limitations describing modern diffraction geometries. As expected for the research in the field of instruments and methods, it also implies a strong cooperation between the two beamlines of SNBL. In 2024 the SNBL new instrumental broadening model has found its way into some of the (main) powder diffraction Rietveld refinement software: namely TOPAS and Profex. It is also clear from the citation list that the new profile function is heavily used by SNBL users and slowly being implemented at many other homelabs and synchrotrons directly impacting the reliability and quality of extracted information. Based on our research the DanMAX beamline has also developed a handy simulation tool, xrdPlanne helping users to simulate realistic diffraction patterns prior to experiment (<https://github.com/LennardKrause/xrdPlanner>).

In a powder diffraction experiment the resolution function defines the instrumental contribution to the peak widths as a function of the Bragg angle. The Caglioti formula stemming from 1958 is frequently applied to model the instrumental broadening and used in structural refinement. The parameters in the Caglioti formula are linked to physically meaningful parameters for most diffraction geometries. However, this link is lost for the now very popular powder diffraction geometry at many beamlines using large 2D area detectors. Here we suggest a new physical model for the instrumental broadening specifically developed for powder diffraction data measured with large 2D area detectors. The model is verified using data from two synchrotron diffraction beamlines with the Pilatus2M and MAR345 detectors. Finally, a functional form is proposed to replace the Caglioti formula for this geometry in the Rietveld method and profile refinements.

First, we show, using error propagation methods, that for large area detectors broadening of Bragg lines contradicts the commonly used Caglioti function.

$$H^2 = U \tan^2 \theta + V \tan \theta + W$$

and a much better model of observed broadening is given by

$$H_{2\Theta}^2 = A \cos^4 2\Theta + B \cos^2 2\Theta + C$$

$$A = \frac{2 \ln 2}{D^2} (p^2 - 2t^2 - c^2), B = \frac{2 \ln 2}{D^2} (2t^2 + 2c^2), C = 2\phi^2 \ln 2.$$

where D is the sample to detector distance, p is the pixel size (or point spread function, if any) of the detector, t is the thickness of detector's sensitive layer, c is size of sample (e.g. diameter of capillary with powder sample), and phi denotes the angular divergence of the scattered beam See figure 1.

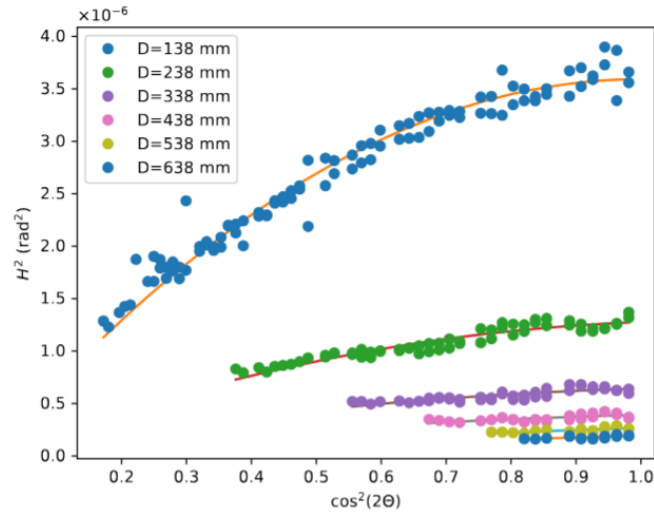


Figure 1 Experimental resolution functions and their fits for various sample-to-detector distances with LaB₆ measured at SNBL BM01 beamline.

Second, starting from the new resolution function for large-area detectors for XRD, we expand this approach into direct space. The effect of instrumental parameters on PDF peak resolution is developed mathematically, then studied with modelling and comparison to experimental PDFs.

- Chernyshov, D., Dyadkin, V., Emerich, H., Valkovskiy, G., McMonagle, C. J., Van Beek, W. *On the resolution function for powder diffraction with area detectors* **Acta Cryst. A** 77, 497-505, 2021
- Chernyshov D, Marshall KP, North ET, Fuller CA, Wragg DS. *Instrumental broadening and the radial pair distribution function with 2D detectors.* **Acta Crystallogr A Found Adv.** 2024 80, 1

Unravelling the components of diffuse scattering using deep learning

A new tool for the analysis of diffuse scattering from a substitutional disorder in molecular crystals reported in (Fuller & Rudden, 2024). We believe that proposed approach, albeit currently limited to binary disorder, will help to simplify analysis of diffuse scattering – one of the major challenges in modern crystallography. Here, a deep-learning method, DSFU-Net, is presented based on the Pix2Pix generative adversarial network, which takes a plane of diffuse scattering as input and factorizes it into the contributions from the molecular form factor and the chemical short-range order. The DSFU-Net was trained on 198421 samples of simulated diffuse scattering data and performed extremely well on the unseen simulated validation dataset in this work. On a real experimental example, DSFU-Net successfully reproduced the two components with a quality sufficient to distinguish between similar structural models based on the form factor and to refine short-range-order parameters, achieving values comparable to other established methods, Figure 1. This new approach could streamline the analysis of diffuse scattering as it requires minimal prior knowledge of the system, allows access to both components in seconds and is able to compensate for small regions with missing data. DSFU-Net is freely available for use and represents a first step towards an automated workflow for the analysis of single crystal diffuse scattering.

To create this ground-breaking tool, Chloe Fuller generated tens of thousands of synthetic training datasets for machine learning, employing an artificial intelligence image recognition algorithm that continuously learns from each newly solved problem. This method not only transforms the structural analysis of disordered materials but also revolutionizes the accumulation of structural knowledge, storing it within the trained network.

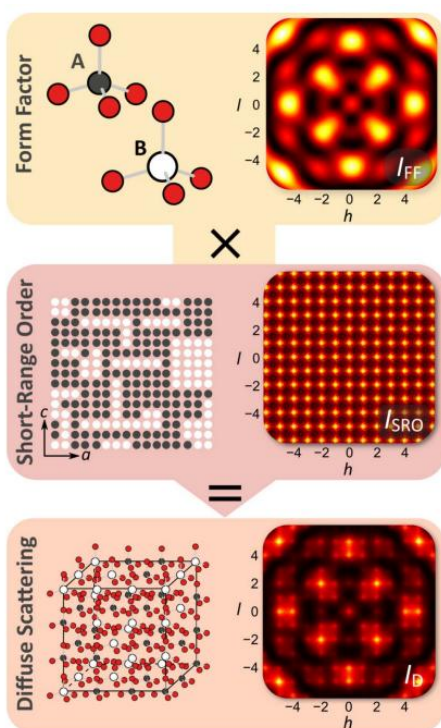


Figure 1 The diffuse scattering components of binary substitutional disorder with one disordered site per unit cell. The site can be occupied by either molecule A or molecule B, as shown in the top panel. Molecule A has a smaller central atom, than the red atoms. The diffuse scattering components of binary substitutional disorder with one disordered site per unit cell. The site can be occupied by either molecule A or molecule B, as shown in the top panel. Molecule A has a smaller central atom, the red atoms sit closer to the central atom and the scattering power is lower than that of molecule B. The difference between their molecular form factors causes structured scattering shown by I_{FF} on the top right panel. The middle panel illustrates Short-Range Order, i.e. whether molecule A is more likely to be found next to molecule B or vice versa. It gives rise to a periodic grid of maxima, I_{SRO}. The bottom panel shows the whole disordered crystal structure and the total diffuse scattering, I_D.

- Fuller, C. A. & Rudden, L. S. P. (2024). *Unravelling the components of diffuse scattering using deep learning*. *IUCr*, 11, 3

Success story: SNBL's software on diffuse scattering using deep learning applied to a user case

Chloe Fuller's tool was successfully applied during a user experiment uniquely describing the structural arrangement of quantum nanodots in a porous framework. Such luminescent clusters, being organized into a regular network, represents a new class of meta-materials with interesting applications; however the regularity of their network is only partial and traditional structural characterization does not provide with any information on the clastr-clastr correlations. The necessary information is however encoded in the diffuse scattering. The work is currently being finalized, preliminary results reported at a few conferences show that application of Chloe Fuller's tool DSFU-Net allows not only to recover the correlations but also help to solve the structure of nanodots.

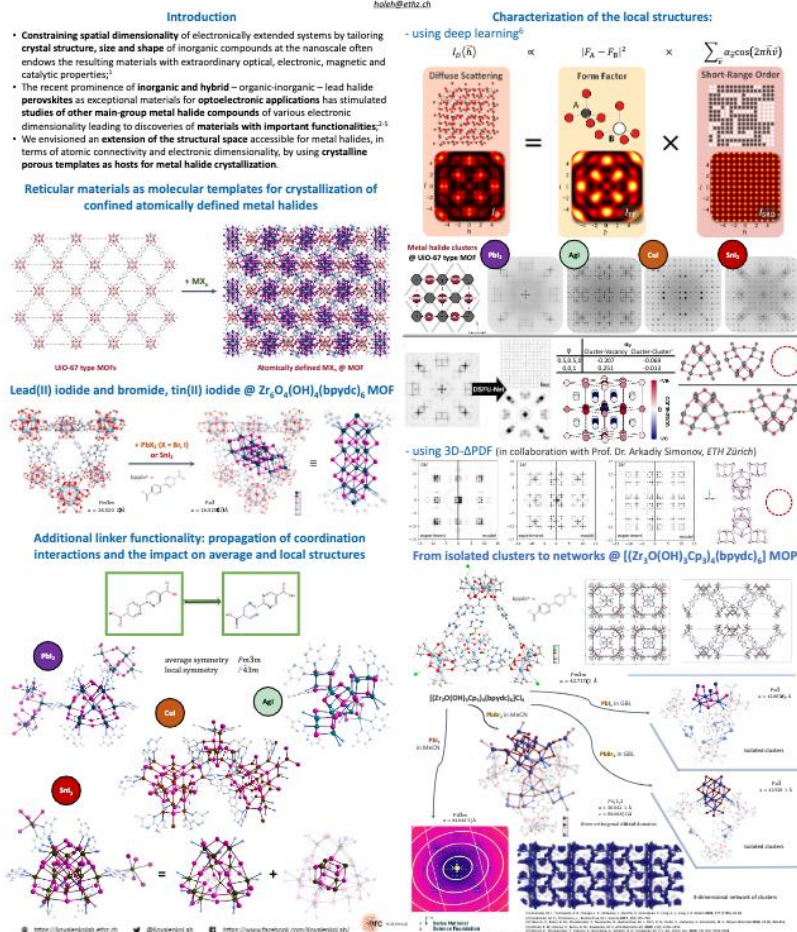
ETH zürich

Empa
Materials Science and Technology

Hybrid Materials of Metal Halide Nano-Sized Clusters Orderly Confined in Single Crystal Metal-Organic Reticular Materials

Oleh Hordichuk^{1,2}, Yurii Okis^{1,2}, Anatolii Kuznetsov^{1,2}, Artem Yanchak^{1,2}, Jean de Montmolin^{1,2},
Chloe Fuller³, Michael Würle³, Dmitry Chernyshov³, Maksym Kovalenko^{1,2}

¹ Laboratory of Inorganic Chemistry, Department of Chemistry and Applied Biosciences, ETH Zürich, Switzerland
² Laboratory for Thin Films and Photovoltaics, Empa – Swiss Federal Laboratories for Materials Science and Technology, Dübendorf, Switzerland
³ Swiss-Norwegian Beamlines at the European Synchrotron Radiation Facility, Grenoble, France
hoh@ethz.ch



SNBL's Outreach

[Spotlight article on the ESRF frontpage](#)

X-ray spectroscopy experiments unravel the transformations of ruthenium catalysts during nitric acid production

Scientists have used the non-invasive technique of *in-situ* X-ray absorption spectroscopy at beamline BM31 to investigate the redox transformations of ruthenium catalysts during the oxidation of nitric oxide to nitrogen dioxide, a key step in the production of nitrate fertilisers for agriculture. A deeper understanding of the process could lead to higher-yield, more efficient fertiliser production.

One of the main objectives in the drive towards more sustainable chemical processes is to intensify the processes themselves, thereby reducing their carbon footprint and increasing energy efficiency. One such example is the oxidation of nitric oxide, one of the main steps in the chemical process that produces industrial nitric acid [1,2]. Nitric acid is a corrosive mineral acid mainly used to produce nitrate fertilisers, which dramatically improve agricultural output in modern agrarian systems. Commercial nitric acid production uses the century-old Ostwald process, which consists of three important chemical steps: catalytic oxidation of ammonia using a Pt-Rh gauze catalyst; followed by gas-phase oxidation of NO to NO₂ using a series of heat exchangers, and finally, NO₂ absorption in water to produce nitric acid. Catalysing the bulky homogeneous gas-phase oxidation of NO to NO₂ may lead to about a 15% intensification of the Ostwald process [1]. Supported Ru catalysts show promising activity and stability at ambient and 4 bar(g) pressures at industrial nitric acid production conditions.

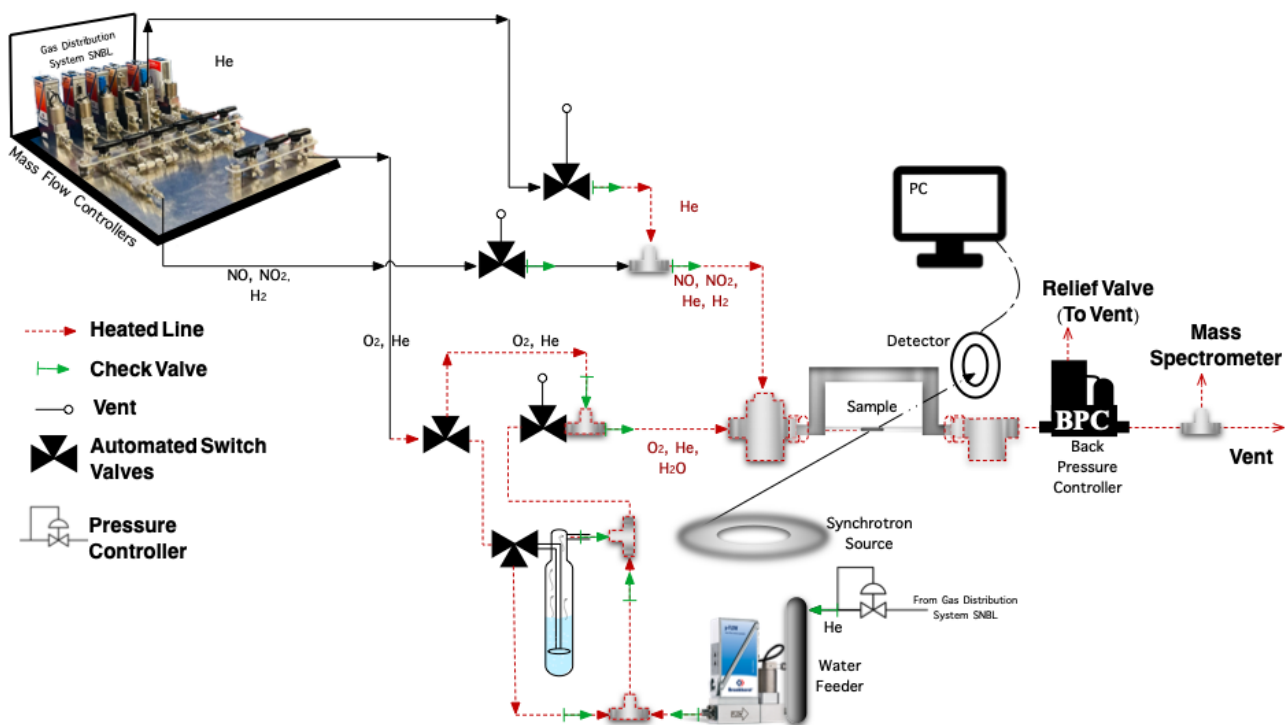


Fig. 1: *In-situ* X-ray absorption experimental setup for oxidation of nitric oxide at beamline BM31.

Experiments at the ESRF have helped to decipher the enigma behind the Ru catalyst's capacity to oxidise nitric oxide at industrially relevant conditions, thus paving the way to intensifying a large established industrial process [1,2]. *In-situ* X-ray absorption spectroscopy (XAS) at the Ru K edge (22.1172 keV) was carried out at

the Swiss-Norwegian beamline (SNBL) BM31. Figure 1 illustrates the experimental setup: X-rays continuously irradiated the γ -Al₂O₃-supported Ru catalyst during NO oxidation. An X-ray absorption near-edge structure (XANES) spectrum was collected every 8-10 seconds, precisely recording the changes in the Ru in the catalyst sample at isothermal conditions. A mass spectrometer (MS) was used to analyse O₂ and NO₂ in the product process gas.

Multivariate curve resolution-alternating least squares (MCR-ALS) data analysis of the *in-situ* XANES data collected during the experiment revealed two distinct components of Ru (as presented in Figure 2a). Component A was completely reduced (representing Ru⁰ in the metallic state) and component B was 30% oxidised. By synchronising the XANES and MS data acquisition rate, subtle changes could be observed in the Ru during NO oxidation. Figures 2c and 2f display the synchronised MCR-ALS contribution plot and the MS signals of O₂ and NO₂ in a 20-minute time frame. The oxidation state of a fraction of Ru in the catalyst oscillates between slightly oxidised and completely reduced. To understand the oscillating behaviour, extended X-ray absorption fine structure (EXAFS) spectroscopy and X-ray photo-electron spectroscopy (XPS) analyses of the two components were performed, and a clear surface oxidation was observed in component B (as presented in Figures 2d and 2e).

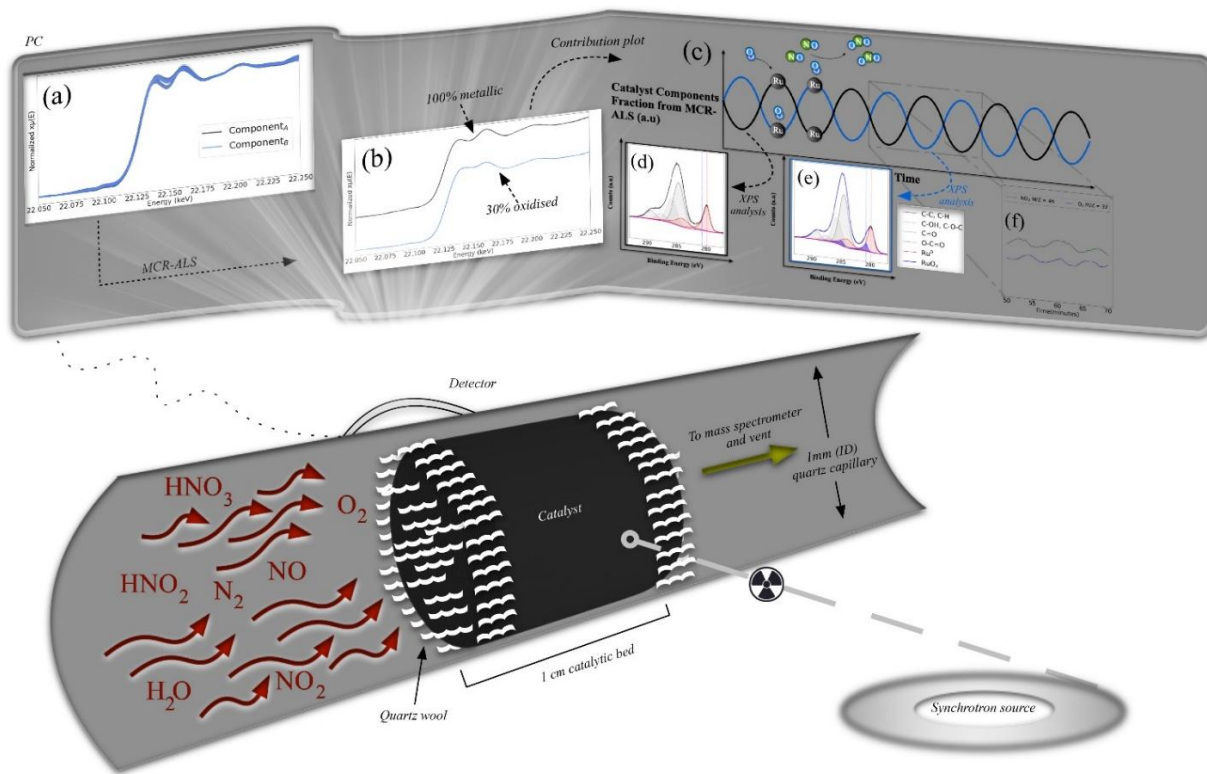


Fig. 2: **a)** γ -Al₂O₃-supported Ru catalysts *in-situ* XANES profiles collected during NO oxidation at 350°C. **b)** MCR-extracted components from the XANES data in **(a)**. **c)** MCR-calculated contribution plot across 3 hours of XANES data collection. **d)** C 1s and Ru 3d XPS spectra of **(d)** component A and **(e)** component B. **f)** Collected mass spectrometer signal for O₂ and NO₂ during 20 minutes of a total of 3 hours NO oxidation. The results reveal the mechanism behind NO oxidation at industrial nitric acid production conditions over γ -Al₂O₃-supported Ru catalysts, and suggest a method to further tune the performance of the Ru catalysts at demanding reaction conditions. Furthermore, the study demonstrates that with careful experimental design

and data analysis from complimentary techniques, a bulk technique such as X-ray absorption spectroscopy can also probe the surface of the sample. Overall, the work highlights the capacity of *in-situ* X-ray tools to bridge the gap between laboratory- and industrial-scale reactions.

Principal publication and authors

Redox transformations of Ru catalyst during NO oxidation at industrial nitric acid production conditions, J. Gopakumar (a), P.M. Benum (a), I.-H. Svenum, (b), B.C. Enger (c), D. Waller (d), M. Rønning (a), *J. Chem. Eng.* **475**, 146406 (2023); <https://doi.org/10.1016/j.cej.2023.146406>

(a) Norwegian University of Science and Technology (NTNU), Department of Chemical Engineering, Trondheim (Norway)

(b) SINTEF Industry, Materials and Nanotechnology group, Trondheim (Norway)

(c) SINTEF Industry, Kinetic, and Catalysis group, Trondheim (Norway)

(d) YARA Technology Center, Porsgrunn (Norway)

References

[1] C. Grande *et al.*, *Ind. Eng. Chem. Res.* **57**, 10180-10186 (2018).

[2] J. Gopakumar *et al.*, *Catal. Sci. Tech.* **13**, 2783-2793 (2023).



Norwegian University of
Science and Technology



Julian Walker wins Sten and Ingrid Ahrlands price

The Ingrid and Sten Ahrlands Prize is awarded every 5 years to a young Nordic researcher who has made outstanding contributions to the field of experimental Chemistry. The price is awarded by the Royal Physiographic Society in Sweden. The society is one of 10 royal scientific societies established by the Swedish King in 1772. The term physiographic was in common use at the time of the Society's founding in 1772 but no longer belongs to our vocabulary. For a number of years now, its secondary title "Academy for the Natural Sciences, Medicine and Technology" is used. The charter of the Society is to promote scientific endeavour in all of these disciplines. Julian was rewarded the price for his career which was strongly leaning on collaborations with SNBL featuring at least 7 publications in the past 5 years. The publications include variable temperature, variable pressure and in situ electric field diffraction measurements of ionic molecular plastic crystals and tetragonal tungsten bronzes.



- Bellosio-Casuso C., de Pedro I., Cañadillas-Delgado L., Beobide G., Sánchez-Andújar M., Ben J.G., Walker J., González Izquierdo P., Cano I., Fernández J.R., Fabelo O. - **Structural and physico-chemical characterization of hybrid materials based on globular quinuclidinium cation derivatives and tetrachloridocobaltate(II) anions**
CrystEngComm **26**, 439-451 (2024)
DOI: 10.1039/d3ce00759f
- Gelpi M., García-Ben J., Rodríguez-Hermida S., López-Beceiro J., Artiaga R., Baaliña Á., Romero-Gómez M., Romero-Gómez J., Zaragoza S., Salgado-Beceiro J., Walker J., McMonagle C.J., Castro-García S., Sánchez-Andújar M., Señaris-Rodríguez M.A., Bermúdez-García J.M. - **Empowering CO2 eco refrigeration with colossal breathing caloric like effects in MOF?508b**
Advanced Materials **36**, 2310499-1-2310499-9 (2024)
DOI: 10.1002/adma.202310499
- Pedersen V.H., Chavez Panduro E.A., Hua W., Michaelsen M.G., Chernyshov D., Walker J., Grande T., Einarsrud M.A. - **Thermal expansion of $Sr_xBa_{1-x}Nb_2O_6$ across and above the ferroelectric phase transition**
Journal of the European Ceramic Society **44**, 907-913 (2024)
DOI: 10.1016/j.jeurceramsoc.2023.10.016

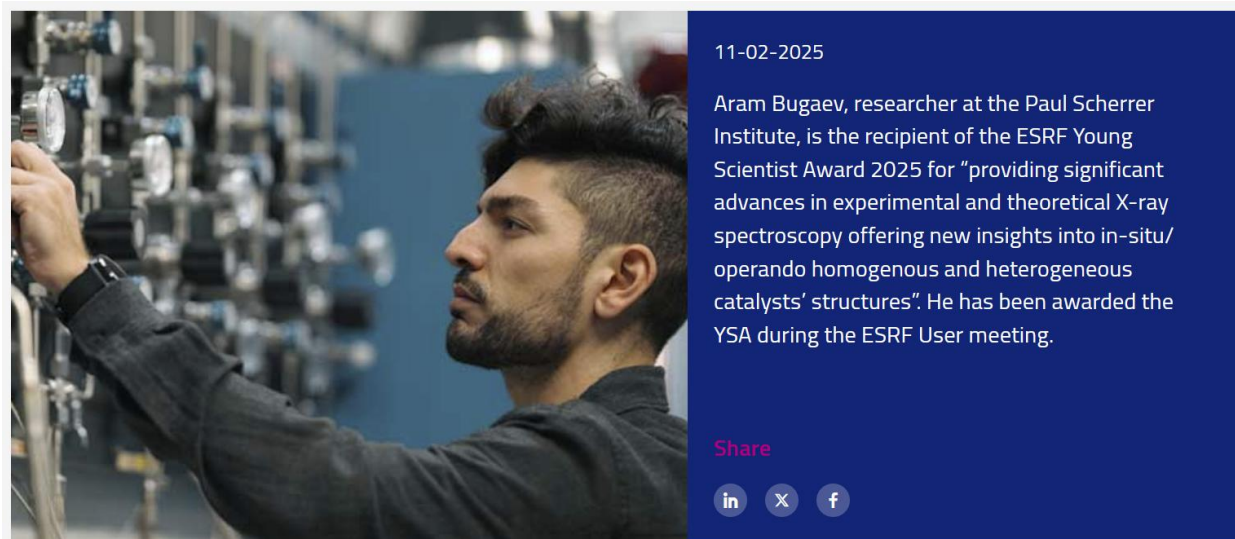
- Dafonte-Rodriguez, P., Delgado-Ferreiro, I., Garcia-Ben, J., Ferradanes-Martinez, A., Gelpi, M., Walker, J., McMonagle, C.J., Castro-Garcia, S., Senaris-Rodriguez, M.A., Bermudez-Garcia, J., Sanchez-Andujar, M. **Exploring the effect of pressure on the crystal structure and caloric properties of the molecular ionic hybrid $[(\text{CH}_3)_3\text{NOH}]_2[\text{CoCl}_4]$**
Chem. Commun., 60, 14065-14068, 2024
DOI: 10.1039/D4CC05125D
- Walker J., Sødahl E.D., Scherre S., Marshall K., Chernyshov D., Berland K., Rojac T. - **Electromechanical properties of uniaxial polar ionic plastic crystal $[(\text{C}_2\text{H}_5)_4\text{N}][\text{FeBrCl}_3]$**
Journal of Physics: Energy 6, 025026-1-025026-14 (2024)
DOI: 10.1088/2515-7655/ad405c
- Walker J., Marshall K.P., Salgado-Beceiro J., Williamson B.A.D., Løndal N.S., Castro-García S., Sánchez Andupr M., Selbach S.M., Chernyshov D., Einarsrud M.A. – **Mesophase transitions in $[(\text{C}_2\text{H}_5)_4\text{N}][\text{FeBrCl}_3]$ and $[(\text{CH}_3)_4\text{N}][\text{FeBrCl}_3]$ ferroic plastic crystals**
Chemistry of Materials 34, 2585-2598 (2022)
DOI: 10.1021/acs.chemmater.1c03778



NTNU

Norwegian University of
Science and Technology

Aram Bugaev wins the ESRF Young Scientist Award 2025



Bugaev specialises in developing experimental and theoretical approaches for operando spectroscopy for catalysis. This includes designing new setups, especially for high pressures and liquid phase reactions, as well as new strategies for data analysis that involve big data and machine learning. “X-ray spectroscopy is my true passion and I do my best to make it accessible and useful for relevant, let’s say real life applications”, explains Bugaev. These include the development of new drugs, green energy and circular economy solutions for our sustainable future.

Bugaev is not a newcomer at the ESRF. Back in 2013, during his masters at the Southern Federal University at Prof. Alexander Soldatov's group and later a PhD in the University of Turin, under the guidance of Carlo Lamberti, he started using beamlines BM23 and the Swiss-Norwegian beamline BM31. “The ESRF has become a huge and integral part of my life and I cannot imagine what my research would look like without ESRF”, he acknowledges.

It is not the first time that Bugaev’s work is awarded. This year, he has received a Swiss National Science Foundation (SNSF) Starting Grant, to design "Microfluidic reactors to uncover structure-performance relationships in heterogenous and homogenous catalysis in flow". In contrast to the classical approach, where scientists create small models of a real reactors, he will develop a series unique devices that will be suitable for both synchrotron studies, as well as industrial large scale production.

Bugaev has a master’s in physics (Nanoscale Structure of Materials) from the Southern Federal University (Russia), a PhD in Chemistry and materials science from the University of Turin (Italy) and a doctoral degree (habilitation) in Physics from the Southern Federal University (Russia) on the topic “Dynamics of the atomic and electronic structure of the palladium-based catalysts under relevant industrial conditions”.

References from his latest work at the ESRF, the first two are exclusively from SNBL's BM31, the third paper is from BM23.

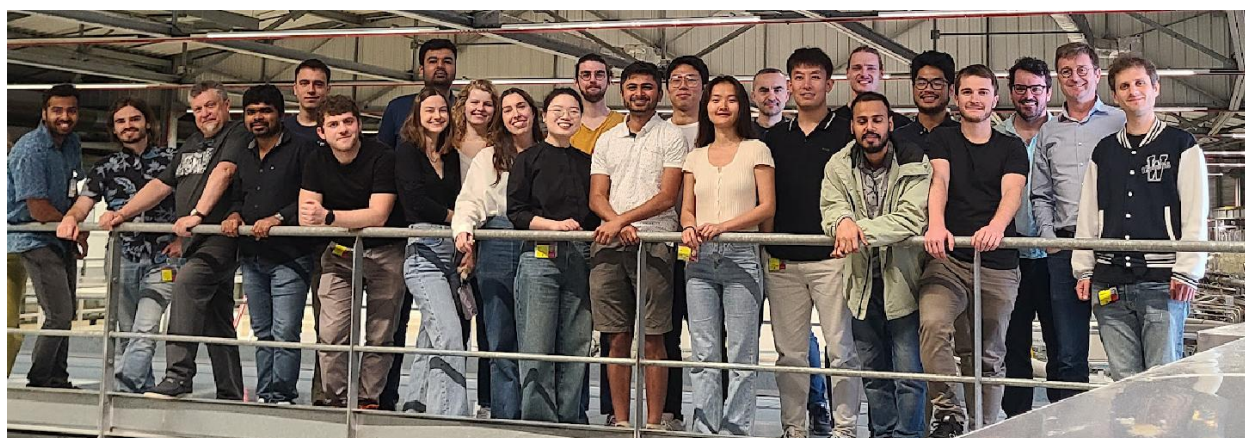
- O. Usoltsev, D. Stoian, A. Skorynina, E. Kozyr, P. N. Njoroge, R. Pellegrini, E. Groppo, J. A. van Bokhoven, A. Bugaev, Restructuring of Palladium Nanoparticles during Oxidation by Molecular Oxygen. *Small* 2024, 20, 2401184. <https://doi.org/10.1002/sml.202401184>
- Skorynina, A.A., Lazzarini, A., Sannes, D.K., Kozyr, E.G., Ahoba-Sam, C., Bordiga, S., Olsbye, U. and Bugaev, A.L., 2024. The structure of Pd-functionalized UiO-67 during CO₂ hydrogenation. *Journal of Materials Chemistry C*, 12(10), pp.3564-3572. <https://doi.org/10.1039/D3TC04175A>
- Beckers, I., Bugaev, A. and De Vos, D., 2023. Dual ligand approach increases functional group tolerance in the Pd-catalysed C–H arylation of N-heterocyclic pharmaceuticals. *Chemical Science*, 14(5), pp.1176-1183. <https://doi.org/10.1039/D2SC04911B>

Text by Montserrat Capellas Espuny



Swiss Summer School on Diffraction and Crystallography, BM01-ESRF

The first Swiss SNBL at ESRF BM01 Summer School on Diffraction and Crystallography was held in Grenoble, 05-09 June 2023. Due to its success, it was repeated the following year from May 13-17, 2024. The school was proposed by Swiss members of the Swiss-Norwegian Council Wendy Lee Queen (EPFL) and Paula Abdala (ETHZ), who also organized financial support and educational certification. Over 40 students from ETHZ and EPFL have attended the schools to explore the theoretical and practical aspects of advanced structural characterization of crystals, powders and thin films. The schools included lectures, tutorials and practical exercises demonstrating the benefits of synchrotron diffraction data for various facets of materials science. During lectures organized by BM01 staff, students got familiar with the basics of synchrotron science, diffraction and crystallography. Particular attention was paid to the information content of diffraction data, data processing, and in-situ and operando experiments. The students also presented their research projects, the presentations followed by discussions on the possible diffraction experiments that could help answer their underlying scientific questions. As part of the practical exercises, the students measured their own samples including in-situ structural evolution of powder materials during a chemical reaction, textured films of MOFs and solar cell compounds, and single crystals with correlated disorder. The students were therefore exposed to a wide variety of projects, and the final lesson was allocated for a discussion on how to write and submit proposals for future synchrotron experiments.



Picture of students of 2nd SNBL summer school

PhD student Ghewa Alsabeh

EPFL Laboratory of Photonics and Interfaces and Smart Energy Materials, Adolphe Merkle Institute, University of Fribourg

“The synchrotron summer school was a one of a kind experience for me! It was the first time I ever saw and worked with such a big and powerful synchrotron. Seeing how these measurements take place in real life was amazing and prepared me well for my next beamtime application and measurements!

Such a high-brilliance photon beam allowed me to learn more information about the perovskites I am studying due to the high accuracy of light diffraction from it. I was able to prove the formation of 2D phase, study the phase purity, the orientation of the materials and get much more information.

Besides this, I had the chance to engage with a team of experts in the field to discuss my project and the obstacles I am facing for a better understanding of my material. Huge thanks go to BM01 staff for their assistance not only during the school but also in the after-school follow-ups!”

Summer school success stories

One of the salient features of the SNBL summer schools is that students are bringing their own samples and together with SNBL staff relevant experiments and are designed and executed on the spot. The students and staff have performed numerous diffraction experiments; diffraction on nanoparticles of High Entropy Alloys (Julia Chmielewska, EMPA), surface scattering from molecular membranes (Kumar Lab, EPFL, Sion), texture analysis of rolled aluminium (Yandong Jing, Thermomechanical Metallurgy Laboratory, EPFL, Neuchâtel), diffraction from MOF-coated wood (Yong Ding, ETH, Zurich) represent the variety of topics. Three publications have been identified with data collected during the summer schools with collaborations spanning out over: EPFL, ETHZ, PSI, EMPA, Rigaku, University of Cambridge and SNBL.

Yong Ding^{ab}, Mahdiah Shakoorioskooie^c, David Mannes^c, Zhidong Zhang^d, Dmitry Chernyshov^e and Ingo Burgert^{ab}, 2025. **Laser-drilled functional wood materials show improved dimensional stability upon humidity changes—a neutron imaging analysis.** *Journal of Materials Chemistry A*.

^aWood Materials Science, Institute for Building Materials, ETH Zürich, 8093, Zürich, Switzerland

^bWoodTec Group, Cellulose & Wood Materials, Empa, 8600 Dübendorf, Switzerland

^cLaboratory for Neutron Scattering and Imaging, PSI Center for Neutron and Muon Sciences, Forschungsstrasse 111, 5232 Villigen, Switzerland

^dDurability of Engineering Materials, Institute for Building Materials, ETH Zurich, 8093 Zurich, Switzerland

^eSwiss-Norwegian Beam Lines at European Synchrotron Radiation Facility, 71 Avenue des Martyrs, Grenoble 38043, France

D'Andria, Matteo^a, Tiago Elias Abi-Ramia Silva^a, Edoardo Consogno^a, Frank Krumeich^b, and Andreas T. Güntner^a. **Metastable CoCu₂O₃ Nanocrystals from Combustion-Aerosols for Molecular Sensing and Catalysis.** *Advanced Materials* 36, no. 47 (2024): 2408888.

^aHuman-Centered Sensing Laboratory Department of Mechanical and Process Engineering, ETH Zurich, Zurich CH-8092, Switzerland

^bLaboratory of Inorganic Chemistry, Department of Chemistry and Applied Biosciences, ETH Zurich, Zurich CH-8093, Switzerland

P. Domingues, Nancy^a, Miriam J. Pougina^a, Yutao Li^a, Elias Moubarak^a, Xin Jin^a, F. Pelin Uran^a, Andres Ortega-Guerrero^{ab}, Christopher P. Ireland^a, Pascal Schouwink^c, Christian Schürmann^d, Jordi Espín^e, Emad Oveisi^f, Fatmah Mish Ebrahim^{ag}, Wendy Lee Queen^e & Berend Smit^a **Unraveling metal effects on CO₂ uptake in pyrene-based metal-organic frameworks.** *Nature Communications* 16, no. 1 (2025): 1516.

^aLaboratory of Molecular Simulation (LSMO), Institut des Sciences et Ingénierie Chimiques, École Polytechnique Fédérale de Lausanne (EPFL), Rue de l'Industrie 17, 1951, Sion, Switzerland

^bNanotech@surfaces Laboratory, Empa - Swiss Federal Laboratories for Materials Science and Technology, 8600, Dübendorf, Switzerland

^cX-ray Diffraction and Surface Analytics Platform, École Polytechnique Fédérale de Lausanne (EPFL), Rue de l'Industrie 17, 1951, Sion, Switzerland

^dRigaku Europe SE, Hugenottenallee 167, 63263, Neu-Isenburg, Germany

^eLaboratory for Functional Inorganic Materials (LFIM), Institut des Sciences et Ingénierie Chimiques, École Polytechnique Fédérale de Lausanne (EPFL), Rue de l'Industrie 17, 1951, Sion, Switzerland

[†]Interdisciplinary Centre for Electron Microscopy (CIME), École Polytechnique Fédérale de Lausanne (EPFL), 1015, Lausanne, Switzerland

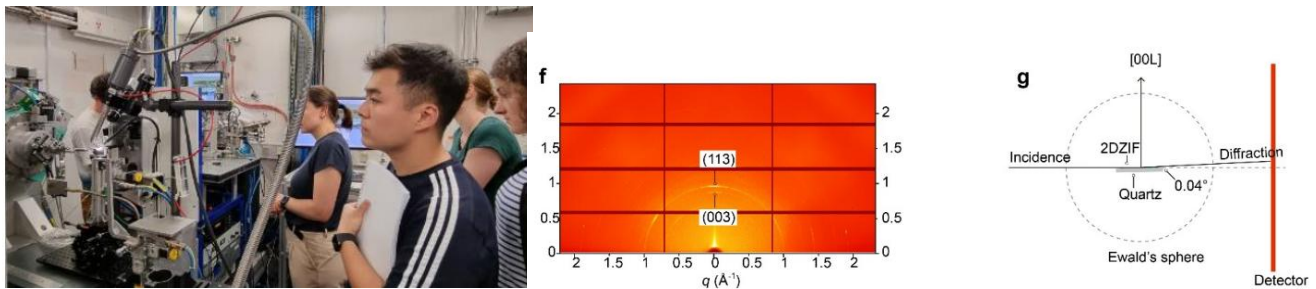
[‡]Cavendish Laboratory, School of Physical Sciences, University of Cambridge, Cambridge, United Kingdom

Summer school success stories continued

SNBL staff has been strongly involved in teaching the next generation of Swiss PhD students at the two summer schools. A tutorial paper (Steele *et. al.* 2023) has been published and lectures are also systematically given at MaMaSELF schools (Master MaMaSELF –Master in Materials Science powERed by Large scale Facilities) illustrating the continuous efforts of attracting and preparing new users in the field of diffraction and crystallography with synchrotron light.

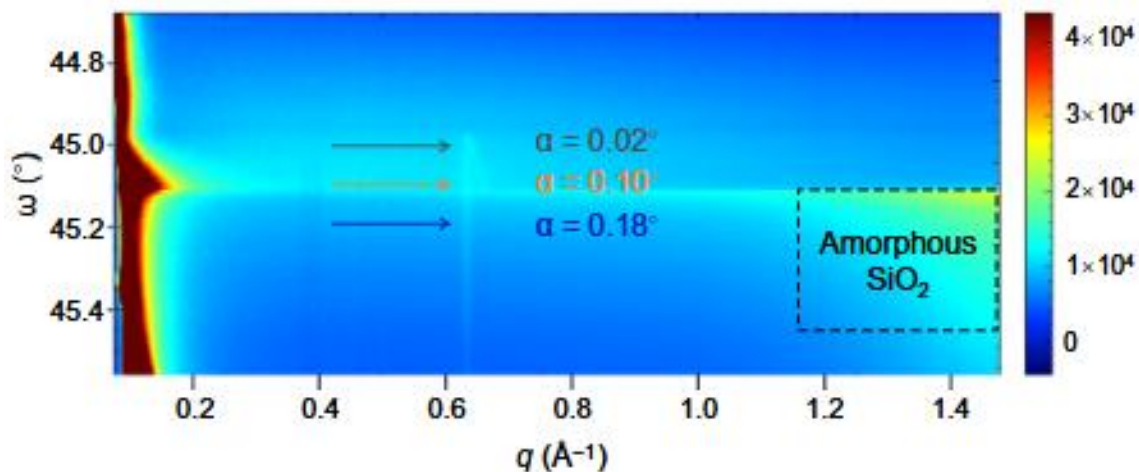
Steele, J.A., Solano, E., Hardy, D., Dayton, D., Ladd, D., White, K., Chen, P., Hou, J., Huang, H., Ali Saha, R., Wang, L., Gao, F., Hofkens, J., Roeffaers, M.B.J., Chernyshov, D., Toney, M.F. *How to GIWAXS: Grazing Incidence Wide Angle X-Ray Scattering Applied to Metal Halide Perovskite Thin Films* **Adv. Energy Mater.**, 13, 27, 2300760, 2023

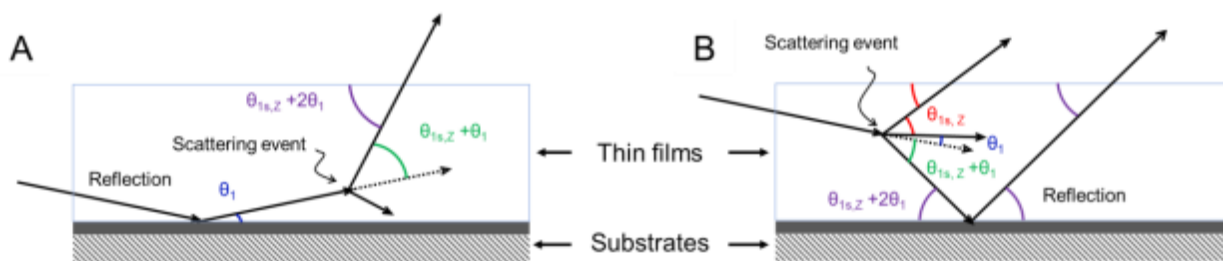
Many students of the EPFL The Laboratory of Advanced Separations (LAS) headed by Prof. Kumar Varoon Agrawal have participated in the SNBL summer schools. The knowledge acquired on GIWAXS experiments has been employed on studying nanometer and unit cell thick membranes resulting in three high profile publication one of which (Liu *et. al.* in Nature materials 2023) was selected as an ESRF highlight in 2023. Meaningful diffraction experiments on such thin and weakly scattering films are only feasible at dedicated synchrotron beamlines such as SNBL. A complete characterization of the films was achieved by combining grating-incidence diffraction with texture analysis, and also powder diffraction of the film materials.



Summer School on Diffraction and Crystallography, BM01- SNBL and GIWAXS experiment at BM01

The quality of the data is best illustrated by the observation of the double-beam effect during in-depth scanning (Song *et al.* Science Advances 2024)





Top: Observation of the double-beam in the upper MOF layer. Bottom: Schematics of the effect illustrating refraction and diffraction inside the film.

Liu, Y. Miao, L. F. Villalobos, S. Li, D. J. Babu, H.-Y. Chi, M. T. Vahdat, J. Hao, Y. Han, M. Tsapatsis, K. V. Agrawal*, "Unit-cell-thick zeolitic imidazolate framework films for membrane application", **Nature Materials**, 2023. DOI: 10.1038/s41563-023-01669-z

Song, Q. Liu, S. Swathilakshmi, H.-Y. Chi, Z. Zhou, R. Goswami, D. Chernyshov, K. V. Agrawal High-performance H₂/CO₂ separation from 4-nm-thick oriented Zn₂(benzimidazole)₄ films. **Science Advances**.10, eads6315(2024). DOI:10.1126/sciadv.ads6315

Heng-Yu Chi, Shuqing Song, Kangning Zhao, Kuang-Jung Hsu, Qi Liu, Yueqing Shen, Anne Faustine Sido Belin, Arthur Allaire, Ranadip Goswami, Wendy L. Queen, and Kumar Varoon Agrawal Non-van-der-Waals Oriented Two-Dimensional UiO-66 Films by Rapid Aqueous Synthesis at Room Temperature **Journal of the American Chemical Society** 2025 147 (9), 7255-7263 DOI: 10.1021/jacs.4c11134

SNBL's international review,

The ESRF organizes an international review every 4 to 5 year for each beamline. SNBL was reviewed at the end of 2024. The previous review was held in 2019.

The panel consisted of:

Professor Jerome Hastings

- SLAC National Accelerator Laboratory, USA
- ESRF Science Advisory Committee
- Chair PSI Photon Science Advisory Committee

Professor Simon R. Bare

- Stanford Synchrotron Radiation Lightsource (SSRL) at SLAC National Accelerator Laboratory, USA

Professor John Evans

- Inorganic Chemistry in the Chemistry Department at the University of Durham, UK

Professor Karen Friese

- Deputy Institute Director Jülich Centre for Neutron Science, Germany
- Professor Crystallography at RWTH Aachen University

Professor Santiago Garcia-Granda

- Full professor of Physical-Chemistry, University of Oviedo, Asturias, Spain
- President of the European Crystallographic Association (ECA)
- President of the Executive Committee of the IUCr

Professor Atsushi Urakawa

- Catalysis Engineering, Technical University Delft, The Netherlands

Their report is provided next.

Beamline Review Panel SNBL BM01/31

Research by Users

The beamline staff presented an exciting range of high-quality scientific outputs in both the written report and during their presentations. We thank them for the quality of information provided. Much of the work is tackling some of the major challenges faced by society around energy storage (e.g. battery materials and electrolytes), energy production (e.g. solar cell materials), and catalysts for cleaner chemical processes such as hydrogen production or CO₂ to methanol conversion. The overall scientific output was impressive in terms of both quantity (1.7 publications per experiment, >480 publications in total) and quality (judged by the journals in which they were published and the citations of several papers). The work has both academic and industrial impact and we note that around 20% of publications in the area of energy and 25% in the area of catalysis came from SNBL in a recent ESRF cross-cutting review. The panel believes that the science areas being tackled are appropriate for these beamlines. We strongly recommend a continued focus in these areas, and continued use of multiple characterisation techniques and multi-length scale analysis.

On BM01 the panel noted high quality work on CsPbI₃ materials for solar cell applications, and how their structure can be controlled by strain engineering. Many of the key insights in this work came from the beamline team's ability to develop grazing incident diffraction experiments and provide bespoke data analysis routines for its interpretation during the experiment. We also noted the exquisite information obtainable from diffuse scattering experiments on the control of defect and pore structure in Prussian Blue analogues.

On BM31 the panel was impressed by a series of publications on CO₂ hydrogenation catalysts which probed their activation, operation and eventual deterioration and by how follow up work by other users had led to significantly-improved systems. We also noted the importance of *operando* studies on battery materials and catalytic reactors, and how the ability to perform spectroscopy (XAS) alongside diffraction and total scattering experiments allows the simultaneous probing of multiple aspects of a materials function. Examples from battery chemistry and catalysis showcased the techniques now available at BM31.

Much of the work is enabled by the exceptional sample environment equipment (furnaces, flow cells, pressure cells, battery cells, electric-field cells) developed by the team with external users. We encourage continued activity in this area.

The beamline is operated as a CRG with 1/3 of the time for Norwegian users, 1/3 for Swiss and 1/3 for general ESRF use. Based on the funding model in place we were satisfied that the CRG time is appropriately allocated, and the figures presented showed that the Swiss/Norwegian usage was sensibly balanced, with all relevant groups having access possibilities. The ESRF-allocated time is enormously over subscribed (7:1) for BM31 and this will doubtless be discouraging people from applying. Given the funding model in place we can't offer any recommendations to change this.

Research by Staff

The staff at SNBL are actively and passionately pursuing outstanding, independent research that has enabled the productive and diverse science generated by both beamlines. It is clear that the staff want the users to succeed in their experiments, and do their best to respond in a timely manner to suggested

Jerome Hastings (SAC member), Simon R Bare, John Evans, Karen Friese, Santiago Garcia-Granda, Atsushi Urakawa

changes in the setup. The staff research starts with the staff discussing and understanding the specific needs of their users and adapting the available instrumentation and sample environment to them. As a result, the staff have implemented a range of the tools and methods which allow the users to be successful in their research. This research spans developing sample environments, understanding the details of detector response, to data processing and analysis. The users have gained substantially as a result of this staff research.

We highlight three examples as illustrations of the excellence of the staff research: (i) the sample environment and (ii) understanding the detailed response of the Pilatus 2M detector., and (iii) interpretation of diffuse scattering. First, the new high temperature, high heating rate, low axial gradient capillary heater has transformed the ability of the user to accurately and reproducibly control the temperature of their sample for both in-situ XRD and XAS measurements. This unique, user-friendly, stable design allows high-temperature measurements (>1000°C) and ramp rates m (>100°C/min). The staff carefully mapped out the response and temperature uniformity of the design. This design gives the users a competitive advantage. (ii) The staff have mapped out the gain response, distortion, cosmic ray interference, and fluorescence response of the Pilatus 2M detector thus allowing for artifact-free data in e.g. PDF at high q . (iii) A further highlight from the research of the staff is the activity aiming at the understanding of diffuse scattering making use of machine-learning techniques and developments aiming at the interpretation of 3D Delta PDFs.

It was clear from all the presentations that the staff respond in real time to requests by the users to implement tools and methods. They are responsive to the changes and needs as the focus of the research shifts to new topics. Given the limited staff and time available the output is outstanding.

Technical Status of the Beamline

BM01 is a good beamline for the *in situ/operando* investigation of single crystals, powders, and thin films with scattering methods and has a highly user-friendly conceptualization. The level of development of the software for the processing of diffraction data is very high and enables an immediate on-the-fly analysis/visualization of the data, of key importance for an efficient realization of the experiments.

BM31 offers an advanced combination of XRD, XAS and PDF. In particular, the multi-absorption edge experimental platform provides fast, automated XAS measurements for samples containing more than one element of interest.

The level of automation on BM31 after the successful upgrade is exceptional and enables users to easily perform complex data collections using the combined techniques available at the beamline (total scattering, XAS). It also allows the straightforward control of the sophisticated sample environment and facilitates the realization of extremely complex experiments. The degree of reproducibility of energy, position and stability of the monochromator is outstanding. If additional resources would become available, BM31 would highly benefit from an upgrade to a multi-element fluorescence detector as this would facilitate the study concentrations of an element, impacting a range of energy/sustainability research.

The technical status of both beamlines is adequate for a 4th generation synchrotron source. Both beamlines are technically state of the art with a very high level of automation. The continuous efforts of the beamline staff in the development of sophisticated sample environments, together with the available multi-technique capabilities, enables the investigation of materials, devices and processes on different length scales.

Jerome Hastings (SAC member), Simon R Bare, John Evans, Karen Friese, Santiago Garcia-Granda, Atsushi Urakawa

BM01 may benefit significantly from the enhanced coherence related to the EBS, in particular with respect to imaging techniques in combination with diffraction experiments. The projected upgrade plans for the beamline will allow the full exploitation of the 2 PW source from the EBS upgrade.

Both beamlines are very user friendly. The staff offers full support to the users starting with help at the stage of proposal writing, the design of experiments, the analysis of the data, all the way to the finished publication. This is reflected in the high quality publication output per user experiment (1.7 publications /experiment). Due to the strong interaction of the users with the beamline staff, there is a well-established long-term (expert) user community. This helps to keep the quality of the beamline's output on a very high level, despite the fact that the available staffing level could/should be improved.

Future Technical Developments

The SNBL suite, BM01 and BM31, were conceived prior to the EBS upgrade. Significant effort has focused on the successful upgrade of BM31 that was recently completed and now provides a unique platform for x-ray spectroscopy and scattering. The only important component missing on BM31 is harmonic rejection and focusing optics. There are, of course, constant needs in specific components as new capabilities become available commercially, for example a multi-element fluorescence detector. These incremental improvements need to be included in the overall development.

Presently, neither beamline has EBS-specific capabilities but the upgrade plan presented for BM01 is focused on EBS-specific features, in particular, the brightness of the x-ray source in the center of the arc. As with the flagship imaging capabilities of the ESRF on BM18, the proposed BM01 upgrade will add imaging capabilities only possible because of the x-ray source characteristics based on the EBS upgrade.

BM31 already has a high degree of automation and provides a suite of x-ray scattering and spectroscopy methods. The BM01 plans extend this to both the simultaneous characterization at multiple length scales using x-ray scattering methods and sequential imaging modalities on the same sample.

The developments of x-ray optics to provide the smallest focal spot sizes will increase time-resolution for the multi-scale scattering techniques, PDF/WAXS/SAXS, and allow for the breadth of imaging modalities present at modern SR sources.

Of course a challenge is how to deal with sample damage (especially with spatially resolved measurements) with the flux density possible with the EBS. This can only be addressed after the BM01 upgrade.

It should be noted that upon the completion of the BM01 upgrade the forefront application of these tools is envisioned to have a 10 year lifetime at a minimum before any major refurbishment would be required.

Staff

The scientific and technical expertise of the beamline staff is central to the successful operation of BM01/BM31. Their skills not only complement each other but are also enhanced through interactions with a robust user community, driving long-term ground-breaking research and high-quality results of societal importance. Despite these strengths, the beamlines are significantly understaffed. Currently, stable and productive operations are maintained through the exceptional motivation, technical

Jerome Hastings (SAC member), Simon R Bare, John Evans, Karen Friese, Santiago Garcia-Granda, Atsushi Urakawa

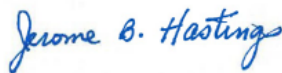
capabilities, and teamwork of the existing staff, who maximize their collective potential through complementary cooperation. Ideally, staffing levels should be increased, particularly as BM01's plan includes imaging capabilities - a development that would likely make additional staffing essential. We noted that the loss of post doctoral staff on the beamlines will likely impact the timely success of long-term innovation and in-house research.

Summary of Recommendations

We strongly support the long-term continuation and development of the outstanding, highly productive scientific capabilities of BM01/BM31, and note their high impact on societally important challenges. These benefit not only Swiss and Norwegian users but also the general ESRF user community as indicated by the extremely high over-subscription of the beamlines.

- To take the best advantage of EBS, we strongly support the upgrade plan of BM01.
- We support the acquisition of a state-of-art multi-element fluorescence detector for BM31 to allow study of low concentration samples.
- We recommend maintaining the leadership in continuing user-inspired, science-driven capabilities such as advanced sample environments.
- We recommend maintaining the leadership in developing tools for the community such as on line analysis and visualization to drive experimental decisions in real time as well as the software to interpret diffuse scattering.
- We recommend one postdoctoral fellow per beamline to make best use of the available beamtime.
- We support maintaining the focus on providing the infrastructure to meet the needs of major societal challenges through continued partnership among industry, academia and beamline staff.
- It should be ensured that resilience/compatibility to changes in control software is maintained.

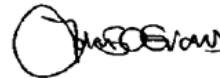
Signatures:



Jerome Hastings



Simon R Bare



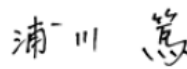
John Evans



Karen Friese



Santiago Garcia-Granda



Atsushi Urakawa

Jerome Hastings (SAC member), Simon R Bare, John Evans, Karen Friese, Santiago Garcia-Granda, Atsushi Urakawa

Scientific output and usage analysis

Impact Factors 2024

79 peer reviewed papers were published in 2024 containing data from SNBL. 38% of the SNBL publications are published in journals with an impact factor above 10 and 56% above impact factor 7. See below the detailed distribution of papers per journal in 2024 and their impact factor.

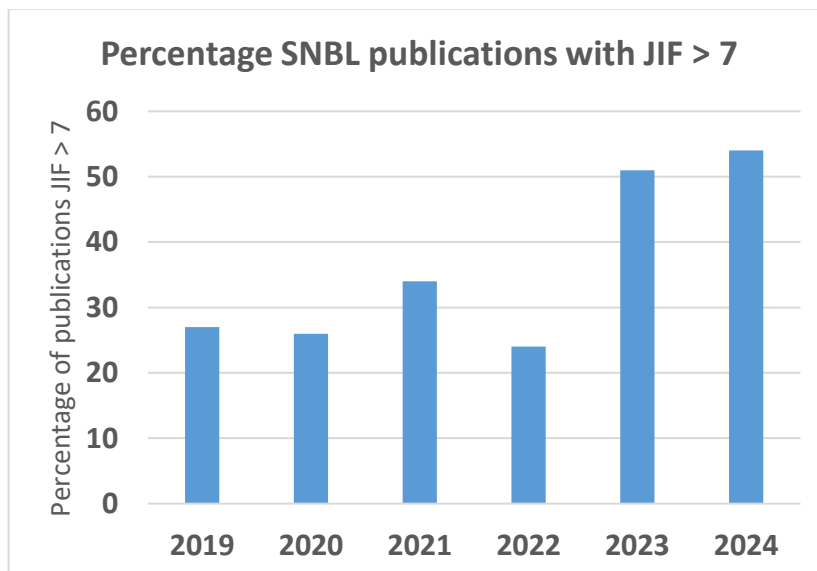
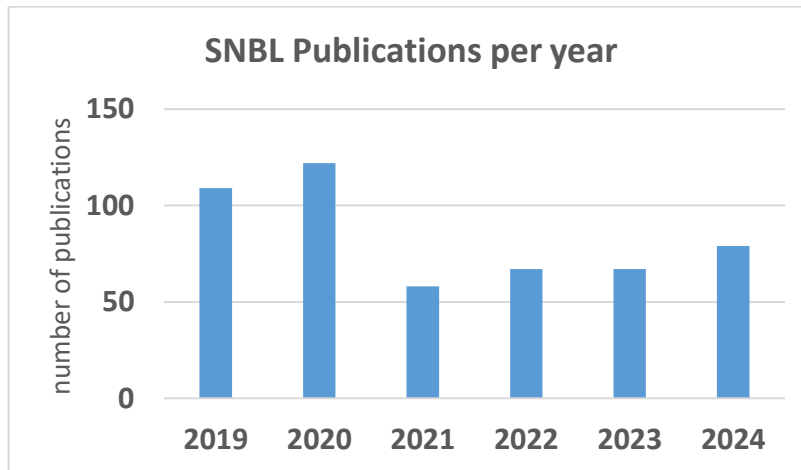
Journal	Web of Science Documents	Journal Impact Factor
NATURE CATALYSIS	2	42.9
NATURE MATERIALS	1	37.2
ENERGY & ENVIRONMENTAL SCIENCE	1	32.4
ADVANCED MATERIALS	4	27.4
ENERGY STORAGE MATERIALS	1	18.9
ADVANCED FUNCTIONAL MATERIALS	1	18.5
ANGEWANDTE CHEMIE-INTERNATIONAL EDITION	2	16.1
ACS NANO	3	15.8
NATURE COMMUNICATIONS	2	14.7
JOURNAL OF THE AMERICAN CHEMICAL SOCIETY	6	14.5
ADVANCED SCIENCE	1	14.3
SMALL	2	13
ACS CATALYSIS	3	11.7
SCIENCE ADVANCES	1	11.7
ACS MATERIALS LETTERS	1	9.9
ACS APPLIED MATERIALS & INTERFACES	1	8.5
CHEMICAL SCIENCE	1	7.6
CHEMSUSCHEM	1	7.5
CHEMISTRY OF MATERIALS	8	7.2
MATERIALS TODAY SUSTAINABILITY	1	7.1
JOURNAL OF PHYSICS-ENERGY	1	7
JOURNAL OF CATALYSIS	1	6.5
JOURNAL OF ALLOYS AND COMPOUNDS	1	5.8
JOURNAL OF THE EUROPEAN CERAMIC SOCIETY	1	5.8
JOURNAL OF MATERIALS CHEMISTRY C	1	5.7
BATTERIES & SUPERCAPS	2	5.1
JOURNAL OF PHYSICAL CHEMISTRY LETTERS	1	4.9
MICROPOROUS AND MESOPOROUS MATERIALS	2	4.8
CATALYSIS SCIENCE & TECHNOLOGY	2	4.4
INORGANIC CHEMISTRY	2	4.3
ADVANCED MATERIALS INTERFACES	1	4.3
CHEMICAL COMMUNICATIONS	2	4.3
MOLECULES	1	4.2
CHEMCATCHEM	1	3.8

ACS OMEGA	1	3.7
APPLIED PHYSICS LETTERS	1	3.5
ADVANCED ENGINEERING MATERIALS	1	3.4
JOURNAL OF PHYSICAL CHEMISTRY C	1	3.3
PHYSICAL REVIEW MATERIALS	1	3.1
PHYSICA E-LOW-DIMENSIONAL SYSTEMS & NANOSTRUCTURES	1	2.9
PHYSICAL CHEMISTRY CHEMICAL PHYSICS	1	2.9
IUCRJ	1	2.9
METALS	1	2.6
CRYSTENGCOMM	1	2.6
ORGANOMETALLICS	1	2.5
JOURNAL OF ELECTROCHEMICAL SCIENCE AND TECHNOLOGY	1	2.2
PHOTONICS	1	2.1
ACTA CRYSTALLOGRAPHICA A-FOUNDATION AND ADVANCES	1	1.9
MENDELEEV COMMUNICATIONS	1	1.8
HELVETICA CHIMICA ACTA	1	1.5
ACTA CRYSTALLOGRAPHICA SECTION B-STRUCTURAL SCIENCE	1	1.3

Summery Impact Factors 2019-2024

The impact from the 20 months EBS upgrade shutdown, starting in Dec 2018, and COVID 19 pandemic starting in March 2020 are inevitably visible in the SNBL output. On the positive side it's also clear the output is starting to pick up both in quantity and quality.

Year	Total Publications	JIF Above > 7	JIF Percentage >7	Average JIF
2024	79	43	54	10.4
2023	67	34	51	8.9
2022	67	16	24	5.7
2021	58	20	34	6.5
2020	122	32	26	5.8
2019	109	29	27	6.2
Total	502	174	36	7.25



Research Areas 2024

All the SNBL papers in 2024 were also categorized by research area. As the earlier years it's clear SNBL has a strong portfolio in energy related research, chemistry and materials science followed by physics and crystallography. See below the full distribution per Research Area.

Research Area	Web of Science Documents
MATERIALS SCIENCE, MULTIDISCIPLINARY	38
CHEMISTRY, PHYSICAL	36
CHEMISTRY, MULTIDISCIPLINARY	35
NANOSCIENCE & NANOTECHNOLOGY	18
PHYSICS, APPLIED	10
PHYSICS, CONDENSED MATTER	9
CRYSTALLOGRAPHY	4
CHEMISTRY, INORGANIC & NUCLEAR	3
ELECTROCHEMISTRY	3
CHEMISTRY, APPLIED	2
ENERGY & FUELS	2
ENGINEERING, CHEMICAL	2
GREEN & SUSTAINABLE SCIENCE & TECHNOLOGY	2
METALLURGY & METALLURGICAL ENGINEERING	2
PHYSICS, ATOMIC, MOLECULAR & CHEMICAL	2
BIOCHEMISTRY & MOLECULAR BIOLOGY	1
CHEMISTRY, ORGANIC	1
ENVIRONMENTAL SCIENCES	1
MATERIALS SCIENCE, CERAMICS	1
OPTICS	1

Scientific output Partner countries 2024

2024	
Institute	Web of Science Documents
ETH Zurich	17
Ecole Polytechnique Federale de Lausanne	12
Paul Scherrer Institute	9
Swiss Federal Laboratories for Materials Science & Technology (EMPA)	8
University of Zurich	4
University of Bern	2
University of Basel	1
ABB	1
Swiss Center for Electronics & Microtechnology (CSEM)	1
University of Fribourg	1

2024	
Institute	Web of Science Documents
University of Oslo	14
Norwegian University of Science & Technology (NTNU)	10
Institute for Energy Technology (IFE)	10
University of Bergen	2
Universitetet i Stavanger	2
SINTEF	2
Norwegian University of Life Sciences	1
Norwegian Metrology Service	1

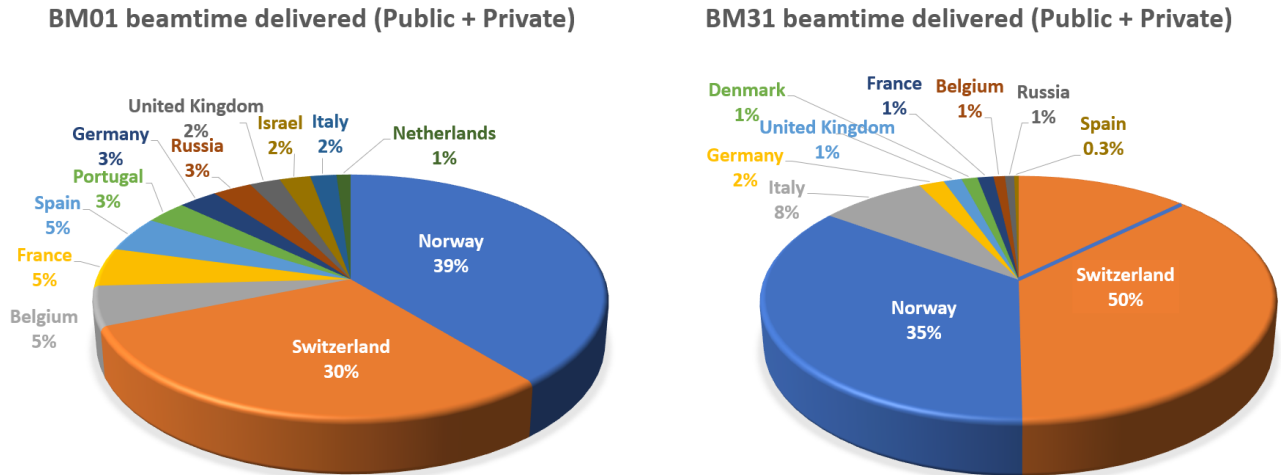
SNBL Scientific output Partner countries 2019-2024

2019-2024	
Name	Web of Science Documents
ETH Zurich	75
Ecole Polytechnique Federale de Lausanne	61
Paul Scherrer Institute (PSI)	37
Swiss Federal Laboratories for Materials Science & Technology (EMPA)	24
University of Geneva	19
University of Zurich	15
University of Bern	6
University of Fribourg	5
Swiss Federal Institute of Aquatic Science & Technology (EAWAG)	3
Swiss Center for Electronics & Microtechnology (CSEM)	3
ABB	2
University of Lausanne	1
University of Basel	1

2019-2024	
Institute	Web of Science Documents
University of Oslo	58
Norwegian University of Science & Technology (NTNU)	43
Institute for Energy Technology (IFE)	37
SINTEF	20
University of Bergen	12
Universitetet i Stavanger	7
Norwegian University of Life Sciences	4
Norwegian Metrology Service	2
Haukeland University Hospital	1
UiT The Arctic University of Tromso	1
Equinor	1

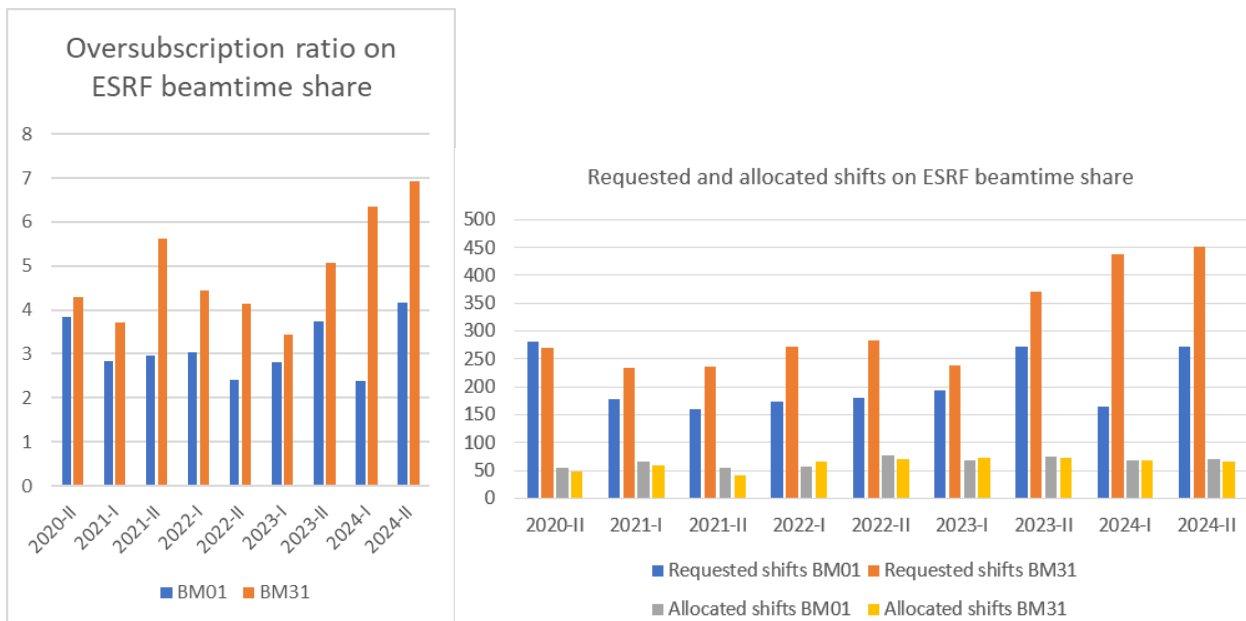
Intensive use of Swiss public ESRF beamtime on BM31

It became very obvious during the statistical analysis of the beamtime usage that Switzerland is heavily using BM31. This analysis was initially performed for the ESRF review. The plot below shows the overall use (public + private beamtime) of SNBL per country.



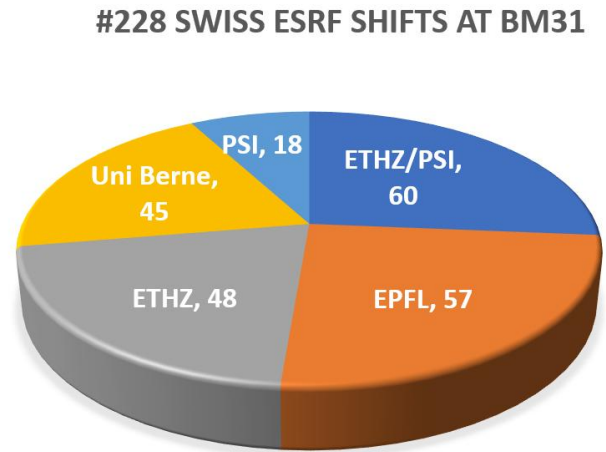
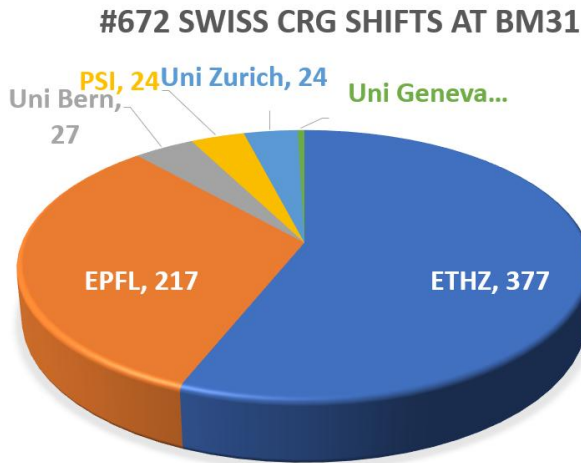
SNBL's BM01 and BM31 overall usage from 2019 to 2024-I (first halve)

Both Norway and Switzerland own 1/3 of the shifts, this private beamtime is granted on scientific merit. The remaining 1/3 of shifts belongs to the ESRF and is an integral part of the ESRF user program. The 50% overall Swiss usage of BM31 clearly indicates that Swiss users must hence be very successful in obtaining public beamtime despite a huge oversubscription on the ESRF beamtime share. From the figure below its obvious that both SNBL beamlines are in extremely high demand, where BM31 is amongst the highest or the highest oversubscribed beamline at the ESRF and beyond.



SNBL's oversubscription ratio's and allocated beamtime

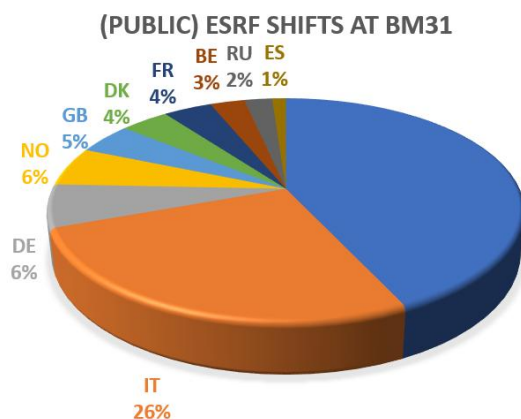
Further analysing and splitting out private and public Swiss use of BM31 it became apparent that some users mainly or only apply for ESRF beamtime. These users are from PSI, the university of Bern or have double affiliations from ETHZ and PSI (see the right side of the figure below).



SNBL's BM31 usage comparing private and public beamtime 2019 to 2024-I (first halve)

It's also interesting to further analyse how the Swiss BM31 usage is represented compared to the overall Swiss share in the ESRF and it turns out that:

- 43% of public ESRF beamtime on BM31 is Swiss
- this 43% represent 10.3% of all Swiss public beamtime at the ESRF
- the 10.3% is consumed on only the 1/3 public share of a beamline on a grand total of 40 equivalent 100% beamlines*¹
- Switzerland has an overall 4% share in the ESRF giving right to 640 shifts/year
- Switzerland has a 1/3 share in SNBL giving right to 150 shifts/year per beamline (BM01 and BM31)
- If the 4% Swiss time would be equally divided over all beamlines, Swiss users would receive 10 times less public time on BM31
- and that in 2023 the 4% Swiss share represents about 4MEuro*²



Member states

- 27.5% France
- 24% Germany
- 13.2% Italy
- 10.5% United Kingdom
- 6% Russia
- 5.8% Benesync (Belgium, The Netherlands)
- 5.0% Nordsync (Denmark, Finland, Norway, Sweden)
- 4% Spain
- 4% Switzerland

*1Note: From the 2023 ESRF highlights one can count that there are physically #49 beamlines at the ESRF but they only provide the equivalent of 40 beamlines in terms of 100% public beamtime availability.

*2Note: One can also find in the 2023 ESRF highlights that members contributed a total of 100.534kEUR with a 4% Swiss share.

REVISED EXPENDITURE AND INCOME BUDGET FOR 2023			
Expenditure	kEUR	Income	kEUR
Accelerator and Source		2023 Members' contributions	100 534,0
Personnel	6 794,0	Funds carried forward from 2022	10 667,0
Recurrent	2 160,0	Other income	
Operating costs	2 010,0	Scientific Associates	7 540,0
Other recurrent costs	150,0	Income from industrial co. activity	3 182,0
Capital	4 756,0	Scientific collaboration and Special projects	7 250,0
Accelerator and Source Devpts	4 756,0	Other concepts/adjustments	-29,0
Beamlines, experiments and in-house research			
Personnel	26 098,0		
Recurrent	6 771,0		
Operating costs	4 971,0		
Other Recurrent costs	1 800,0		
Capital	24 494,0		
Beamline developments	24 494,0		
Technical and administrative supports			
Personnel	33 859,0		
Recurrent	15 940,0		
Capital	8 272,0		
TOTAL	129 144,0	TOTAL	129 144,0

Member states

- 27.5% France
- 24% Germany
- 13.2% Italy
- 10.5% United Kingdom
- 6% Russia
- 5.8% Benesync (Belgium, The Netherlands)
- 5.0% Nordsync (Denmark, Finland, Norway, Sweden)
- 4% Spain
- 4% Switzerland

Involvement of industry in SNBL's 2024 publication output

One of the criteria to measure the industrial relevance of research done is SNBL is to evaluate the number of companies involved in SNBL publications. It turns out that fourteen different companies are involved in a total of seventeen papers. In 2024 roughly one out of five SNBL publications had an industrial partner.

O. Usoltsev, D. Stoian, A. Skorynina, E. Kozyr, P. N. Njoroge, R. Pellegrini, E. Groppo, J. A. van Bokhoven, A. Bugaev, *Restructuring of Palladium Nanoparticles during Oxidation by Molecular Oxygen*. *Small* 2024, 20, 2401184.

<https://doi.org/10.1002/sml.202401184>



Anders Brennhagen, Casper Skautvedt, Carmen Cavallo, David S. Wragg, Alexey Y. Kopolov, Anja O. Sjøstad, and Helmer Fjellvåg *Unraveling the (De)sodiation Mechanisms of BiFeO₃ at a High Rate with Operando XRD* *ACS Applied Materials & Interfaces* 2024 16 (10), 12428-12436

DOI: 10.1021/acsami.3c17296



Frida Sveen Hempel, Wojciech A. Sławiński, Bjørnar Arstad, and Helmer Fjellvåg *Superstructure of Locally Disordered Na₂Zn₂TeO₆* *Chemistry of Materials* 2024 36 (22), 11084-11094 DOI:

10.1021/acs.chemmater.4c01953



Lars F. Lundegaard, Izar Capel Berdiell, Nico König, Nicolai Haaber Junge, Pablo Beato, Dmitry Chernyshov, Stian Svelle, David S. Wragg, *Tracking deactivation of zeolite beta with and without a detailed structure model: XRD analysis and in situ studies* *Microporous and Mesoporous Materials*, Volume 366, 2024,

<https://doi.org/10.1016/j.micromeso.2023.112911>.

TOPSOE

M. Gelpi, J. García-Ben, S. Rodríguez-Hermida, J. López-Beceiro, R. Artiaga, Á. Baaliña, M. Romero-Gómez, J. Romero-Gómez, S. Zaragoza, J. Salgado-Beceiro, J. Walker, C. J. McMonagle, S. Castro-García, M. Sánchez-Andújar, M. A. Señarís-Rodríguez, J. M. Bermúdez-García, *Empowering CO₂ Eco-Refrigeration With Colossal Breathing-Caloric-Like Effects in MOF-508b*. *Adv. Mater.* 2024, 36, 2310499.
<https://doi.org/10.1002/adma.202310499>



Anders Brennhagen, Amalie Skurtveit, David S. Wragg, Carmen Cavallo, Anja O. Sjøstad, Alexey Y. Kuposov, and Helmer Fjellvåg *(De)sodiation Mechanism of Bi₂MoO₆ in Na-Ion Batteries Probed by Quasi-Simultaneous Operando PDF and XAS* *Chemistry of Materials* 2024 36 (15), 7514-7524
DOI: 10.1021/acs.chemmater.4c01503



Lukas Lätsch, Christoph J. Kaul, Alexander V. Yakimov, Rhaïna McEntee, Trees De Baerdemaeker, Andrei-Nicolae Parvulescu, Karsten Seidel, J. Henrique Teles, and Christophe Copéret *Nature of Reactive Sites in TS-1 from 15N Solid-State NMR and Ti K-Edge X-Ray Absorption Spectroscopic Signatures Upon Pyridine Adsorption* *Journal of the American Chemical Society* 2024 146 (43), 29675-29683
DOI: 10.1021/jacs.4c10604



Wei Zhou, Enzo Brack, Christian Ehinger, James Paterson, Jamie Southouse, and Christophe Copéret *Reactivity Switch of Platinum with Gallium: From Reverse Water Gas Shift to Methanol Synthesis* *Journal of the American Chemical Society* 2024 146 (15), 10806-10811
DOI: 10.1021/jacs.4c01144



V. Giulimondi, M. Vanni, S. Damir, T. Zou, S. Mitchell, F. Krumeich, A. Ruiz-Ferrando, N. López, J.J. Gata-Cuesta, G. Guillén-Gosálbez, J.J. Smit, P. Johnston, and J. Pérez-Ramírez *Convergent Active Site Evolution in Platinum Single Atom Catalysts for Acetylene Hydrochlorination and Implications for Toxicity Minimization* ACS Catalysis 2024 14 (18), 13652-13664
DOI: 10.1021/acscatal.4c03533



Colin Hansen, Wei Zhou, Enzo Brack, Yuhao Wang, Chunliang Wang, James Paterson, Jamie Southouse, and Christophe Copéret *Decoding the Promotional Effect of Iron in Bimetallic Pt–Fe-nanoparticles on the Low Temperature Reverse Water–Gas Shift Reaction* Journal of the American Chemical Society 2024 146 (40), 27555-27562
DOI: 10.1021/jacs.4c08517



Lukas Lätsch, Imke B. Müller, Christoph J. Kaul, Trees De Baerdemaeker, Andrei-Nicolae Parvulescu, Karsten Seidel, J. Henrique Teles, Natalia Trukhan, and Christophe Copéret *Formation and Stability of μ_2 -Peroxo on Titanosilicates, Anatase, and Rutile: Implications for Zeotype Catalysts* The Journal of Physical Chemistry C 2024 128 (13), 5553-5558
DOI: 10.1021/acs.jpcc.3c08292



Othman, Mostafa and Jeangros, Quentin and Jacobs, Daniel A. and Futscher, Moritz H. and Zeiske, Stefan and Armin, Ardalan and Jaffrès, Anaël and Kuba, Austin G. and Chernyshov, Dmitry and Jenatsch, Sandra and Züfle, Simon and Ruhstaller, Beat and Tabean, Saba and Wirtz, Tom and Eswara, Santhana and Zhao, Jiashang and Savenije, Tom J. and Ballif, Christophe and Wolff, Christian M. and Hessler-Wyser, Aïcha *Alleviating nanostructural phase impurities enhances the optoelectronic properties device performance and stability of cesium-formamidinium metal–halide perovskites* Energy Environ. Sci.2024 17-11 3832-3847
pub10.1039/D4EE00901K



P. Castro-Fernández, A. I. Serykh, M. Yarar, D. Mance, P. M. Abdala, C. Copéret, A. Fedorov, C. R. Müller, *The Relation between Nature and Stability of H₂-Dissociating Sites and Propene Selectivity in Silica-Supported (Ga,Al)₂O₃ Mixed Oxide Propane Dehydrogenation Catalysts* Helv. Chim. Acta 2024, 107, e202400076.
<https://doi.org/10.1002/hlca.202400076>



Filippo Tavormina, Eleonora Quadri, Paolo Biagini, Riccardo Po, Rosamaria Marrazzo, Maria Antonietta Loi, Luisa Barba, Norberto Masciocchi, and Antonietta Guagliardi *Crystal Orientation, Strain, and Microstrain of Perovskite Films in a Complex Compositional Parameter Space* Chemistry of Materials 2024 36 (18), 8880-8893
DOI: 10.1021/acs.chemmater.4c01714



Sexton, A., Kanters, M., Demchenko, H., Pacáková, B., Fossum, J.O., Balzano, L. and Knaapila, M. *Classifying Tensile Loading History of Continuous Carbon Fiber Composites Using X-Ray Scattering and Machine Learning*. *Adv. Eng. Mater.*, (2024), 26: 2301415.
<https://doi.org/10.1002/adem.202301415>



Taras V. Sekh, Ihor Cherniukh, Etsuki Kobiyama, Thomas J. Sheehan, Andreas Manoli, Chenglian Zhu, Modestos Athanasiou, Marios Sergides, Oleksandra Ortikova, Marta D. Rossell, Federica Bertolotti, Antonietta Guagliardi, Norberto Masciocchi, Rolf Erni, Andreas Othonos, Grigorios Itskos, William A. Tisdale, Thilo Stöferle, Gabriele Rainò, Maryna I. Bodnarchuk, and Maksym V. Kovalenko *All-Perovskite Multicomponent Nanocrystal Superlattices ACS Nano* **2024** 18 (11), 8423-8436
DOI: 10.1021/acsnano.3c13062



P. Domingues, Nancy, Miriam J. Pougin, Yutao Li, Elias Moubarak, Xin Jin, F. Pelin Uran, Andres Ortega-Guerrero, Christopher P. Ireland, Pascal Schouwink, Christian Schürmann, Jordi Espín, Emad Oveisi, Fatmah Mish Ebrahim, Wendy Lee Queen & Berend Smit *Unraveling metal effects on CO₂ uptake in pyrene-based metal-organic frameworks*. *Nature Communications* 16, no. 1 (2025): 1516.
DOI:10.1038/s41467-025-56296-w



Publication list 2024

1. Abdala P., Müller C. *Uncovering atomic-scale dynamics in solid catalysts via X-ray-based methods* [Chimia 78, 297-303, 2024](#)
2. Albertini P.P., Newton M.A., Wang M., Segura Lecina O., Green P.B., Stoian D.C., Oveisi E., Loiudice A., Buonsanti R. *Hybrid oxide coatings generate stable Cu catalysts for CO₂ electroreduction* [Nature Materials 23, 680-687, 2024](#)
3. Alekseeva O.A., Naberezhnov A.A., Koroleva E.Y., Fokin A.V. *The role of thermal vibrations in transformation of structure transition for sodium nitrate in a restricted geometry* [Physica E 156, 115855-1-115855-6, 2024](#)
4. Almakî, M., Alsabeh, G., Ruiz-Preciado, M.A., Zhang, H., Galerne, M., Moulin, E., Eickemeyer, F.T., Zakeeruddin, S.M., Milic, J.V., Giuseppone, N., Grätzel, M. *Triarylamine Trisamide Interfacial Modulation for Perovskite Photovoltaics* [Adv. Mater. Interfaces, 11, 34, 2301053, 2024](#)
5. Amanullah, S., Cao, W., Brack, E., Plodinec, M., Copéret, C. *Surface Coordination Chemistry of Graphitic Carbon Nitride from Ag Molecular Probes* [Ang. Chemie, 64, 5, e202417428, 2024](#)
6. Artuk K., Turkyay D., Mensi M.D., Steele J.A., Jacobs D.A., Othman M., Chin X.Y., Moon S.J., Tiwari A.N., Hessler-Wyser A., Jeangros Q., Ballif C., Wolff C.M. *A universal perovskite/C60 interface modification via atomic layer deposited aluminum oxide for perovskite solar cells and perovskite-silicon tandems* [Advanced Materials 36, 21, 2311745, 2024](#)
7. Balagurov A.M., Bobrikov I.A., Chernyshov D.Y., Sohatsky A.S., Sumnikov S.V., Yerzhanov B., Golovin I.S. *Tetragonal phases in Fe-Ga alloys: A quantitative study* [Physical Review Materials 8, 073604-1-073604-13, 2024](#)
8. Belloso-Casuso C., de Pedro I., Cañadillas-Delgado L., Beobide G., Sánchez-Andújar M., Ben J.G., Walker J., González Izquierdo P., Cano I., Fernández J.R., Fabelo O. *Structural and physico-chemical characterization of hybrid materials based on globular quinuclidinium cation derivatives and tetrachloridocobaltate(II) anions* [CrystEngComm 26, 439-451, 2024](#)
9. Bercha, S., Rathod, S., Zavorotynska, O., Chavan, S.M. *Probing Ce- and Zr-Fumarate Metal–Organic Framework Formation in Aqueous Solutions with In Situ Raman Spectroscopy and Synchrotron X-ray Diffraction* [ACS Omega, 9, 44, 44321-44335, 2024](#)
10. Bodnarchuk M.I., Feld L.G., Zhu C., Boehme S.C., Bertolotti F., Avaro J., Aebli M., Mir S.H., Masciocchi N., Erni R., Chakraborty S., Guagliardi A., Rainò G., Kovalenko M.V. *Colloid alaziridium lead bromide quantum dots* [ACS Nano 18, 5684-5697, 2024](#)
11. Brennhagen A., Skautvedt C., Cavallo C., Wragg D.S., Kuposov A.Y., Sjøstad A.O., Fjellvåg H. *Unraveling the (de)sodiation mechanisms of BiFeO₃ at a high rate with operando XRD* [ACS Applied Materials & Interfaces 16, 12428-12436, 2024](#)
12. Brennhagen A., Skurtveit A., Wragg D.S., Cavallo C., Sjøstad A.O., Kuposov A.Y., Fjellvåg H. *(De)sodiation mechanism of Bi₂MoO₆ in Na-ion batteries probed by quasi-simultaneous operando PDF and XAS* [Chemistry of Materials 36, 7514-7524, 2024](#)
13. Castro-Fernández P., Serykh A.I., Yarar M., Mance D., Abdala P.M., Copéret C., Fedorov A., Müller C.R. *The relation between nature and stability of H₂-dissociating sites and propene selectivity in silica supported (Ga,Al)₂O₃ mixed oxide propane dehydrogenation catalysts* [Helvetica Chimica Acta 107, 8, e202400076, 2024](#)
14. Chen B., Fan D., Pinto R.V., Dovgaliuk I., Nandi S., Chakraborty D., García-Moncada N., Vimont A., McMonagle C.J., Bordonhos M., Al Mohtar A., Cornu I., Florian P., Heymans N., Daturi M., De Weireld G., Pinto M., Nouar F., Maurin G., Mouchaham G., Serre C. *A scalable robust microporous Al-MOF for post-combustion carbon capture* [Advanced Science 11, 21, 2401070, 2024](#)

15. Chen Z.X., Serykh A.I., Kierzkowska A., Gajan D., Docherty S.R., Yakimov A.V., Abdala P.M., Copéret C., Florian P., Fedorov A., Müller C.R. *Reversible transformation of sub-nanometer Ga-based clusters to isolated [4] Ga(4Si) sites creates active centers for propane dehydrogenation* [Catalysis Science & Technology](#) **14**, 379-390, 2024
16. Chernyshov, D., Marshall, K.P., North, E.T., Fuller, C.A., Wragg, D.S. *Instrumental broadening and the radial pair distribution function with 2D detectors* [Acta Cryst.](#), **A80**, 358-366, 2024
17. D'Andria, M., Abi-Ramia Silva, T.E., Consogno, E., Krumeich, F., Güntner, A.T. *Metastable CoCu₂O₃ Nanocrystals from Combustion-Aerosols for Molecular Sensing and Catalysis* [Adv. Mater.](#), **36**, 47, 2408888, 2024
18. Da Silva, V.R., Fjellvåg, Ø.S., Pokle, A., Hauback, B.C., Deledda, S. *Effect of Carbon Addition and Mechanical Activation on FeNi Alloys for Permanent Magnet Applications* [Metals](#), **14**, 1125, 2024
19. Dafonte-Rodríguez, P., Delgado-Ferreiro, I., Garcia-Ben, J., Ferradanes-Martinez, A., Gelpi, M., Walker, J., McMonagle, C.J., Castro-García, S., Senaris-Rodríguez, M.A., Bermudez-García, J., Sanchez-Andujar, M. *Exploring the effect of pressure on the crystal structure and caloric properties of the molecular ionic hybrid [(CH₃)₃NOH]₂[CoCl₄]* [Chem. Commun.](#), **60**, 14065-14068, 2024
20. Danmo F.H., Westermoen A., Marshall K., Stoian D., Grande T., Glaum J., Selbach S.M. *High-entropy hexagonal manganites for fast oxygen absorption and release* [Chemistry of Materials](#) **36**, 2711-2720, 2024
21. Dempsey E.K., Cumby J. *Mixed anion control of negative thermal expansion in a niobium oxyfluoride* [Chemical Communications](#) **60**, 2548-2551, 2024
22. Fjellvåg Ø.S., Fjellvåg H. *Sn(SO₄)₂·2H₂O from synchrotron powder data* [IUCrData](#), **9**, 12, x241179, 2024
23. Fjellvåg Ø.S., Gonano B., Bernal F.L.M., Amedi S.B., Lyu JK., Pomjakushin V., Medarde M., Chernyshov D., Marshall K., Valldor M., Fjellvåg H., Hauback B.C. *Order-to-disorder transition and hydrogen bonding in the Jahn-Teller active NH₄CrF₃ fluoroperovskite* [Inorg.Chem.](#), **63**, 23, 10594-10602, 2024
24. Fuller C.A., Rudden L.S.P. *Unravelling the components of diffuse scattering using deep learning* [IUCrJ](#) **11**, 34-44, 2024
25. Gawryluk, D.J., Klein, Y.M., Scatena, R., Shang, T., Sibille, R., Sheptyakov, D., Casati, N., Linden, A., Chernyshov, D., Kozłowski, M., Dłuzewski, P., Rossell, M.D., Macchi, P., Medarde, M. *Magnetostructural Coupling at the Néel Point in YNiO₃ Single Crystals* [Chem. Mater.](#), **36**, 16, 7811-7821, 2024
26. Ge Y., Zou T., Martin A.J., Block T., Pöttgen R., Pérez-Ramirez J. *Defective zirconia promotes monometallic iron catalysts for higher alcohol synthesis* [Chem Catalysis](#) **4**, 6, 101010, 2024
27. Gelpi M., García-Ben J., Rodríguez-Hermida S., López-Beceiro J., Artiaga R., Baaliña Á., Romero-Gómez M., Romero-Gómez J., Zaragoza S., Salgado-Beceiro J., Walker J., McMonagle C.J., Castro-García S., Sánchez-Andujar M., Señaris-Rodríguez M.A., Bermúdez-García J.M. *Empowering CO₂ eco refrigeration with colossal breathing caloric like effects in MOF-508b* [Advanced Materials](#) **36**, 16, 2310499, 2024
28. Giulimondi, V., Vanni, M., Damir, S., Zou, T., Mitchell, S., Krumeich, F., Ruiz-Ferrando, A., Lopez, N., Gata-Cuesta, J.J., Guillen-Gosalbez, G., Smit, J.J., Johnston, P., Perez-Ramirez, J. *Convergent Active Site Evolution in Platinum Single Atom Catalysts for Acetylene Hydrochlorination and Implications for Toxicity Minimization* [ACS Catal.](#), **14**, 18, 13652-13664, 2024
29. Hansen, C., Zhou, W., Brack, E., Wang, Y., Wang, C., Paterson, J., Southouse, J., Copéret, C. *Decoding the Promotional Effect of Iron in Bimetallic Pt-Fe-nanoparticles on the Low Temperature Reverse Water-Gas Shift Reaction* [J. Am. Chem. Soc.](#), **146**, 40, 27555-27562, 2024
30. Hempel, F.S., Slawinski, W.A., Arstad, B., Fjellvåg, H. *Superstructure of Locally Disordered Na₂Zn₂TeO₆* [Chem. of Mater.](#), **36**, 22, 11084-11094, 2024

31. Hölderle T., Monchak M., Baran V., Kriele A., Mühlbauer M.J., Dyadkin V., Rabenbauer A., Schökel A., Ehrenberg H., Müller-Buschbaum P., Senyshyn A. *Thermal structural behavior of electrochemically lithiated graphite (LixC6) anodes in Li-ion batteries* [Batteries & Supercaps, 7, 3, e202300499, 2024](#)
32. Houllberghs, M., Radhakrishnan, S., Chandran, C.V., Morais, A.F., Martens, J.A., Breynaert, E. *Harnessing Nuclear Magnetic Resonance Spectroscopy to Decipher Structure and Dynamics of Clathrate Hydrates in Confinement: A Perspective* [Molecules, 29, 14, 3369, 2024](#)
33. Huang H., Zhao J., Guo H., Weng B., Zhang H., Saha R.A., Zhang M., Lai F., Zhou Y., Juan R.Z., Chen P.C., Wang S., Steele J.A., Zhong F., Liu T., Hofkens J., Zheng Y.M., Long J., Roeyffers M.B.J. *Noble metal free high entropy alloy nanoparticles for efficient solar driven photocatalytic CO2 reduction* [Advanced Materials 36, 26, 2313209, 2024](#)
34. Jin F., Fadillah L., Nguyen H.Q., Sandvik T.M., Liu Y., García-Martín A., Salagre E., Michel E.G., Stoian D., Marshall K., van Beek W., Redhammer G., Mehraj Ud Din M., Rettenwander D. *Elucidating the impact of Li3InCl6-coated LiNi0.8Co0.15Al0.05O2 on the electro-chemo-mechanics of Li6PS5Cl-based solid-state batteries* [Chemistry of Materials 36, 6017-6026, 2024](#)
35. Jin, F., Kwon, C., Bugaev, A., Karakurt, B., Lin, Y.-C., Savereide, L., Zhong, L., Boureau, V., Safonova, O., Kim, S., Luterbacher, J.S. *Atom-by-atom design of Cu/ZrOx clusters on MgO for CO2 hydrogenation using liquid-phase atomic layer deposition* [Nature Catalysis, 7, 1199-1212, 2024](#)
36. Justin A., Espín J., Pougin M.J., Stoian D., Schertenleib T., Mensi M., Kochetygov I., Ortega-Guerrero A., Queen W.L. *Post-synthetic covalent grafting of amines to NH2-MOF for post-combustion carbon capture* [Advanced Functional Materials, 34, 7, 2307430, 2024](#)
37. Klag L., Baumgarten L., Gaur A., Sheppard T.L., Grunwaldt J.D. *Comparison of structure and reactivity of hydrothermally prepared Bi-Mo-Co-Fe-O catalysts in selective propylene and isobutene oxidation* [ChemCatChem 16, 8, e202301470, 2024](#)
38. Klimova, N., Snigirev, A. *Diffraction Losses in a Stack of Diamond X-Ray Lenses* [Photonics, 11, 1097, 2024](#)
39. Kuriganova A., Leontyev I., Leontyev N., Smirnova N. *Pt catalysts prepared via top-down electrochemical approach: synthesis methodology and support effects* [Journal of Electrochemical Science and Technology 15, 345-352, 2024](#)
40. Kuriganova A., Smirnova N. *New Insights into Controlling the Functional Properties of Tin Oxides-Based Materials* [J. of Electrochemistry, 31, 2408261, 2024](#)
41. Landuyt, A., Kochetygov, I., McMonagle, C.J., Kumar, P.V., Yuwono, J.A., Queen, W.L., Abdala, P.M., Müller, C.R. *Role of Na2CO3 as Nucleation Seeds to Accelerate the CO2 Uptake Kinetics of MgO-Based Sorbents* [JACS Au, 4, 12, 4809-4820, 2024](#)
42. Lätsch, L., Guda S.A., Romankov V., Wartmann C., Neudorfl J.M., Dreiser J., Berkessel A., Guda A.A., Copéret C. *Tracking coordination environment and reaction intermediates in homogeneous and heterogeneous epoxidation catalysts via Ti L2,3-edge near-edge X-ray absorption fine structures* [J. Am.Chem. Soc., 146, 11, 7456-7466, 2024](#)
43. Lätsch, L., Kaul, C.J., Yakimov, A.V., McEntee, R., De Baerdemaeker, T., Parvulescu, A.N., Seidel, K., Teles, J.H., Copéret, C. *Nature of Reactive Sites in TS-1 from 15N Solid-State NMR and Ti K-Edge X-Ray Absorption Spectroscopic Signatures Upon Pyridine Adsorption* [J. Am. Chem. Soc., 146, 43, 29675-29683, 2024](#)
44. Lätsch, L., Müller I.B., Kaul C.J., De Baerdemaeker T., Parvulescu A.N., Seidel K., Teles J.H., Trukhan N., Copéret C. *Formation and stability of μ_2 -peroxo on titanosilicates, anatase, and rutile: implications for zeotype catalysts* [J. Phys.Chem. C 128, 13, 5553-5558, 2024](#)
45. Li, S., Zhang, Z., Marks, W.R., Huang, X., Chen, H., Stoian, D.C., Erni, R., Triana, C.A., Patzke, G.R. *{Co4O4} Cubanes in a conducting polymer matrix as bio-inspired molecular oxygen evolution catalysts* [Nat. Commun.,15, 8432, 2024](#)

46. Lundegaard L.F., Berdiell I.C., König N., Junge N.H., Beato P., Chernyshov D., Svelle S., Wragg D.S. *Tracking deactivation of zeolite beta with and without a detailed structure model: XRD analysis and in situ studies* [Microporous and Mesoporous Materials 366, 112911, 2024](#)
47. Makarova I.P., Selezneva E.V., Tolstikhina A.L., Gainutdinov R.V. *Regular relations of the composition, structure and properties of crystals of hydrogen-containing compounds* [Lithosphere \(Russia\) 24, 398-405, 2024](#)
48. McMonagle C.J., Fuller C.A., Hupf E., Malaspina L.A., Grabowsky S., Chernyshov D. *Lattice response to the radiation damage of molecular crystals: Radiation-induced versus thermal expansivity* [Acta Crystallographica B 80, 13-18, 2024](#)
49. Muscarella, L.A. *Unveiling the impact of stress: a dynamic twist on properties in halide-perovskites* [Proc. SPIE 13123, Organic, Hybrid, and Perovskite Photovoltaics XXV, 131230B, 2024](#)
50. Negri C., Colombo R., Bracconi M., Atzori C., Donazzi A., Lucotti A., Tommasini M., Maestri M. *Operando UV-vis spectroscopy for real-time monitoring of nanoparticle size in reaction conditions: A case study on rWGS over Au nanoparticles* [Catalysis Science & Technology 14, 1318-1327, 2024](#)
51. Othman M., Jeangros Q., Jacobs D.A., Futscher M.H., Zeiske S., Armin A., Jaffrès A., Kuba A.G., Chernyshov D., Jenatsch S., Züfle S., Ruhstaller B., Tabean S., Wirtz T., Eswara S., Zhao J., Savenije T.J., Ballif C., Wolff C.M., Hessler-Wyser A. *Alleviating nanostructural phase impurities enhances the optoelectronic properties, device performance and stability of cesium-formamidinium metal-halide perovskites* [Energy & Environmental Science 17, 3832-3847, 2024](#)
52. Patzke, G.R., Keller, F., Iannuzzi, M., Reith, L., Marshall, K.P., van Beek, W., Triana, C.A. *Structure-Selection Dynamics of Cobalt Nanoparticles from Solution Synthesis and Their Impact on the Oxygen Evolution Reaction* [ACS Nano, 18, 52, 35533-35549, 2024](#)
53. Pazos Urrea M., Meilinger S., Herold F., Gopakumar J., Tusini E., De Giacinto A., Zimina A., Grunwaldt J.D., Chen D., Rønning M. *Aqueous phase reforming over platinum catalysts on doped carbon supports: Exploring Platinum?Heteroatom interactions* [ACS Catalysis 14, 4139-4154, 2024](#)
54. Pedersen V.H., Chavez Panduro E.A., Hua W., Michaelsen M.G., Chernyshov D., Walker J., Grande T., Einarsrud M.A. *Thermal expansion of $Sr_xBa_{1-x}Nb_2O_6$ across and above the ferroelectric phase transition* [Journal of the European Ceramic Society 44, 907-913, 2024](#)
55. Pereñíguez R., Ferri D. *In situ XRD and operando XRD-XANES study of the regeneration of $LaCo_0.8Cu_0.2O_3$ perovskite for preferential oxidation of CO* [Materials Today Sustainability 27, 100867, 2024](#)
56. Pinheiro Araújo T., Giannakakis G., Morales-Vidal J., Agrachev M., Ruiz-Bernal Z., Preikschas P., Zou T., Krumeich F., Willi P.O., Stark W.J., Grass R.N., Jeschke G., Mitchell S., López N., Pérez-Ramirez J. *Low-nuclearity CuZn ensembles on ZnZrOx catalyze methanol synthesis from CO₂* [Nature Communications 15, 3101, 2024](#)
57. Reim I., Occhipinti G., Törnroos K.W., Jensen V.R. *Pursuing e-selective olefin metathesis: Tuning steric and electronic properties of S,N-chelated ruthenium alkylidenes* [Organometallics 43, 726-736, 2024](#)
58. Ribeiro, C., Tan, B., Figueira, F., Mendes, R.F., Calbo, J., Valente, G., Escamilla, P., Almeida Paz, F.A., Rocha, J., Dinca, M., Souto, M. *Mixed Ionic and Electronic Conductivity in a Tetrathiafulvalene-Phosphonate Metal–Organic Framework* [J. Am. Chem. Soc., 147, 1, 63-68, 2024](#)
59. Roth, J., Trukhina, O., Allouss, D., Stoian, D.C., Schertenleib, T., Felder, T., Queen, W.L. *Post-Synthetic Modification of a MOF via Continuous Flow Methods for Gold E-Waste Recycling* [ChemSusChem, 18, 5, e202401642, 2024](#)
60. Sadovnikov A.A., Boytsova O.V. *Observing the formation of TiO₂ mesocrystals from NH₄TiOF₃ microparticles using in situ thermo-WAXS measurements* [Mendeleev Communications 34, 226-228, 2024](#)
61. Saha D., Slawinski W.A., Kumar S., Fjellvåg H. *Local symmetry deviation from the average structure of MnAs revealed by pair distribution function* [Inorg.Chem., 63, 33, 15503-15509, 2024](#)

62. Salusso D., Ticali P., Stoian D., Wang S., Fan W., Morandi S., Borfecchia E., Bordiga S. *Deciphering local structural complexity in Zn/Ga-ZrO₂ CO₂ hydrogenation catalysts* [Journal of Physical Chemistry Letters](#) **15**, 4494-4500, 2024
63. Schertenleib T., Karve V.V., Stoian D., Asgari M., Trukhina O., Oveisi E., Mensi M., Queen W.L. *A post-synthetic modification strategy for enhancing Pt adsorption efficiency in MOF/polymer composites* [Chemical Science](#) **15**, 8323-8333, 2024
64. Schweigart, P., Hua, W., Sanchez, P.A., Lian, C., Nylund, I.-E., Wragg, D., Lai, S.Y., Cova, F., Svensson, A.M., Blanco, M.V. *Deciphering the Impact of Current, Composition, and Potential on the Lithiation Behavior of Si-Rich Silicon-Graphite Anodes* [Small](#), **21**, 4, 2406615, 2024
65. Sekh T.V., Cherniukh I., Kobiyama E., Sheehan T.J., Manoli A., Zhu C., Athanasiou M., Sergides M., Ortikova O., Rossell M.D., Bertolotti F., Guagliardi A., Masciocchi N., Erni R., Othonos A., Itskos G., Tisdale W.A., Stöferle T., Rainò G., Bodnarchuk M.I., Kovalenko M.V. *All-perovskite multicomponent nanocrystal superlattices* [ACS Nano](#) **18**, 8423-8436, 2024
66. Sexton A., Kanters M., Demchenko H., Pacáková B., Fossum J.O., Balzano L., Knaapila M. *Classifying tensile loading history of continuous carbon fiber composites using X-ray scattering and machine learning* [Adv. Eng. Mater.](#), **26**, 2, 2301415, 2024
67. Shraer S., Dembitskiy A., Trussov I., Komayko A., Aksyonov D., Luchinin N., Morozov A., Pollastri S., Aquilanti G., Ryazantsev S., Nikitina V., Abakumov A., Antipov E., Fedotov S. *Designing a 3D framework NaVOPO₄ as a high-power, low-strain and long-life positive electrode material for Na-ion batteries* [Energy Storage Materials](#) **68**, 103358, 2024
68. Skorynina A.A., Lazzarini A., Sannes D.K., Kozyr E.G., Ahoba-Sam C., Bordiga S., Olsbye U., Bugaev A.L. *The structure of Pd-functionalized UiO-67 during CO₂ hydrogenation* [Journal of Materials Chemistry C](#) **12**, 3564-3572, 2024
69. Skurtveit, A., North, E.T., Park, H., Chernyshov, D., Wragg, D.S., Kuposov, A.Y. *Stepwise Structural Relaxation in Battery Active Materials* [ACS Materials Lett.](#), **7**, 1, 343-349, 2024
70. Song, S., Liu, Q., Swathilakshmi, S., Chi, H.-Y., Zhou, Z., Goswami, R., Chernyshov, D., Agrawal, K.V. *High-performance H₂/CO₂ separation from 4-nm-thick oriented Zn₂(benzimidazole)₄ films* [Sci. Adv.](#), **10**, 50, eads6315, 2024
71. Tavormina, F., Quadrivi E., Biagini, P., Po, R., Marrazzo, R., Loi, M.A., Barba, L., Masciocchi, N., Guagliardi, A. *Crystal Orientation, Strain, and Microstrain of Perovskite Films in a Complex Compositional Parameter Space* [Chem. Mater.](#), **36**, 18, 880-8893, 2024
72. Thogersen, R.V., Hval, H.H., Fjellvag, H. *Elucidation of the Reaction Mechanisms in Antifluorite-Type Li_{5+x}Fe_{1-x}Co_xO₄ Positive Electrodes for Li-Ion Batteries* [Batteries & Supercaps](#), **7**, 9, e202400348, 2024
73. Usoltsev, O., Stoian, D., Skorynina, A., Kozyr, E., Njoroge, P. N., Pellegrini, R., Groppo, E., van Bokhoven, J. A., Bugaev, A. *Restructuring of Palladium Nanoparticles during Oxidation by Molecular Oxygen* [Small](#), **20**, 2401184, 2024
74. Usteri M.E., Giannakakis G., Bugaev A., Pérez-Ramirez J., Mitchell S. *Understanding and controlling reactivity patterns of Pd₁@C₃N₄-catalyzed Suzuki Miyaura couplings* [ACS Catalysis](#) **14**, 12635-12646, 2024
75. Vandenabeele D., Doppelhammer N., Radhakrishnan S., Chandran C V., Jakoby B., Kirschhock C., Breyneart E. *Can the combination of in situ differential impedance spectroscopy and 27Al NMR detect incongruent zeolite crystallization?* [Microporous and Mesoporous Materials](#) **374**, 113141-1-113141-6, 2024
76. Vávra J., Ramona Gaétan P. L., Dattila F., Kormányos A., Priamushko T., Albertini Petru P., Loidice A., Cherevko S., López N., Buonsanti R. *Solution-based Cu⁺ transient species mediate the reconstruction of copper electrocatalysts for CO₂ reduction* [Nature Catalysis](#) **7**, 89-97, 2024

77. Walker J., Sødahl E.D., Scherre S., Marshall K., Chernyshov D., Berland K., Rojac T. *Electromechanical properties of uniaxial polar ionic plastic crystal [(C₂H₅)₄N][FeBrCl₃]* [Journal of Physics: Energy 6, 025026-1-025026-14, 2024](#)
78. Yartys V.A., Akselrud L.G., Denys R.V., Vajeeston P., Ouladdiaf B., Dankelman R., Plomp J., Koldemir A., Schumacher L., Kremer R.K., Pöttgen R., Wragg D.S., Eggert B.G.F., Berezovets V. *Crystal, magnetic structures, and bonding interactions in the TiNiSi-type hydride CeMgSnH: Experimental and computational studies* [Chemistry of Materials 36, 6257-6268, 2024](#)
79. Yartys V.A., Denys R.V., Akselrud L.G., Vajeeston P., Dankelman R., Plomp J., Block T., Pöttgen R., Wragg D., Fisher Eggert B.G., Berezovets V. *Structure and bonding in TiNiSi type LaMgSnH intermetallic hydride* [Journal of Alloys and Compounds 976, 173198-1-173198-10, 2024](#)
80. Zavorotynska, O., Asland, A.C., Dietzel, P.D., Chavan, S.M. *Exploring cluster formation in Zr-MOF synthesis in situ using X-ray absorption spectroscopy* [Phys. Chem. Chem. Phys., 26, 27019-27033, 2024](#)
81. Zaza, L., Stoian, D.C., Bussel, N., Albertini, P.P., Leemans, J., Kumar, K., Loiudice, A., Buonsanti, R. *Increasing Precursor Reactivity Enables Continuous Tunability of Copper Nanocrystals from Single-Crystalline to Twinned and Stacking Fault-Lined* [J. of the American Chemical Society, 146, 47, 32766-32776, 2024](#)
82. Zhang, H., Klimpel, M., Wiecezrak, K., Dubey, R., Okur, F., Michler, J., Jeurgens, L.P.H., Chernyshov, D., van Beek, W., Kravchyk, K.V., Kovalenko, M.V. *Unveiling Surface Chemistry of Ultrafast-Sintered LLZO Solid-State Electrolytes for High-Performance Li-Garnet Solid-State Batteries* [Chem. of Mater., 36, 22, 2024](#)
83. Zhao Y., Wan W., Erni R., Pan L., Patzke G.R. *Operando spectroscopic monitoring of metal chalcogenides for overall water splitting: new views of active species and sites* [Ang. Chemie Inter. Ed., 63,24, e202400048, 2024](#)
84. Zhou W., Brack E., Ehinger C., Paterson J., Southouse J., Copéret C. *Reactivity switch of platinum with gallium: From reverse water gas shift to methanol synthesis* [Journal of the American Chemical Society 146, 10806-10811, 2024](#)
85. Zhou, W., Hansen, C., Cao, W., Brack, E., Docherty, S.R., Ehinger, C., Wang, Y., Wang, C., Copéret, C. *Gallium: A Universal Promoter Switching CO₂ Methanation Catalysts to Produce Methanol* [JACS Au, 5, 1, 217-224, 2024](#)
86. Zimmerli N.K., Rochlitz L., Checchia S., Müller C.R., Copéret C., Abdala Paula M., Abdala P.M. *Structure and role of a Ga-promoter in Ni-based catalysts for the selective hydrogenation of CO₂ to methanol* [JACS Au 4, 237- 252, 2024](#)
87. Zou T., Araújo T.P., Agrachev M., Jin X., Krumeich F., Jeschke G., Mitchell S., Pérez-Ramirez J. *Design of technical ZnO/ZrO₂ catalysts for CO₂ hydrogenation to green methanol* [Journal of Catalysis, 430, 115344, 2024](#)